MIT Joint Program on the
Science and Policy of Global Change

The MIT Integrated Global System Model (IGSM)
Version 2: *Model Description and Baseline Evaluation*

*A.P. Sokolov, C.A. Schlosser, S. Dutkiewicz, S. Paltsev, D.W. Kicklighter,
H.D. Jacoby, R.G. Prinn, C.E. Forest, J. Reilly, C. Wang, B. Felzer,
M.C. Sarofim, J. Scott, P.H. Stone, J.M. Melillo and J. Cohen*

Report No. 124
July 2005

The MIT Joint Program on the Science and Policy of Global Change is an organization for research, independent policy analysis, and public education in global environmental change. It seeks to provide leadership in understanding scientific, economic, and ecological aspects of this difficult issue, and combining them into policy assessments that serve the needs of ongoing national and international discussions. To this end, the Program brings together an interdisciplinary group from two established research centers at MIT: the Center for Global Change Science (CGCS) and the Center for Energy and Environmental Policy Research (CEEPR). These two centers bridge many key areas of the needed intellectual work, and additional essential areas are covered by other MIT departments, by collaboration with the Ecosystems Center of the Marine Biology Laboratory (MBL) at Woods Hole, and by short- and long-term visitors to the Program. The Program involves sponsorship and active participation by industry, government, and non-profit organizations.

To inform processes of policy development and implementation, climate change research needs to focus on improving the prediction of those variables that are most relevant to economic, social, and environmental effects. In turn, the greenhouse gas and atmospheric aerosol assumptions underlying climate analysis need to be related to the economic, technological, and political forces that drive emissions, and to the results of international agreements and mitigation. Further, assessments of possible societal and ecosystem impacts, and analysis of mitigation strategies, need to be based on realistic evaluation of the uncertainties of climate science.

This report is one of a series intended to communicate research results and improve public understanding of climate issues, thereby contributing to informed debate about the climate issue, the uncertainties, and the economic and social implications of policy alternatives. Titles in the Report Series to date are listed on the inside back cover.

Henry D. Jacoby and Ronald G. Prinn,
Program Co-Directors

For more information, please contact the Joint Program Office

Postal Address: Joint Program on the Science and Policy of Global Change
77 Massachusetts Avenue
MIT E40-428
Cambridge MA 02139-4307 (USA)

Location: One Amherst Street, Cambridge
Building E40, Room 428
Massachusetts Institute of Technology

Access: Phone: (617) 253-7492
Fax: (617) 253-9845
E-mail: globalchange@mit.edu
Web site: http://MIT.EDU/globalchange/

Printed on recycled paper

MIT Integrated Global System Model (IGSM) Version 2:
Model Description and Baseline Evaluation

Andrei P. Sokolov, C. Adam Schlosser, Stephanie Dutkiewicz, Sergey Paltsev, David W. Kicklighter, Henry D. Jacoby, Ronald G. Prinn, Chris E. Forest, John Reilly, Chien Wang, Benjamin Felzer, Marcus C. Sarofim, Jeff Scott, Peter H. Stone, Jerry M. Melillo and Jason Cohen

Abstract

The MIT Integrated Global System Model (IGSM) is designed for analyzing the global environmental changes that may result from anthropogenic causes, quantifying the uncertainties associated with the projected changes, and assessing the costs and environmental effectiveness of proposed policies to mitigate climate risk. This report documents Version 2 of the IGSM, which like the previous version, includes an economic model for analysis of greenhouse gas and aerosol precursor emissions and mitigation proposals, a coupled atmosphere-ocean-land surface model with interactive chemistry, and models of natural ecosystems. In this global framework the outputs of the combined anthropogenic and natural emissions models provide the driving forces for the coupled atmospheric chemistry and climate models. Climate model outputs then drive a terrestrial model predicting water and energy budgets, CO_2, CH_4, and N_2O fluxes, and soil composition, which feed back to the coupled climate/chemistry model.

The first version of the integrated framework (which we will term IGSM1) is described in Prinn et al. (1999) and in publications and Joint Program Reports and Technical Notes provided on the Program's website (http://mit.edu/globalchange/). Subsequently, upgrades of component model capabilities have been achieved, allowing more comprehensive and realistic studies of global change. Highlights of these improvements include: a substantially improved economics model, needed to provide emissions projections and to assess an increasingly complex policy environment; a new global terrestrial model comprised of state-of-the-art biogeophysical, ecological and natural biogeochemical flux components, which provides an improved capacity to study consequences of hydrologic and ecologic change; the addition of a three-dimensional ocean representation, replacing the previous two-dimensional model, which allows examination of the global thermohaline circulation and its associated climate change impacts; the addition of an explicit oceanic carbon cycle including the impact of the biological pump; the addition of a new urban air pollution model enabling better treatments of human health and climate impacts; and the addition of greater flexibility for study of terrestrial ecosystem and urban pollution effects. This report documents the essential features of the new IGSM structure.

Contents

1. INTRODUCTION

Projections of climate change over the next century have been hampered by limits to our understanding of, and ability to model, the complex interdependencies of the human-climate system. Among factors contributing to this difficulty are significant uncertainties in climate system properties that determine its response to transient forcing, such as climate sensitivity and the rate at which the deep ocean absorbs heat and carbon dioxide (CO_2). There are additional uncertainties in the forcing itself, especially in the indirect forcing by aerosols (IPCC, 2001). Unfortunately, the available directly-measured ocean, land and atmospheric data for the 20th century can only place limited constraints on these key quantities (Andronova & Schlesinger, 2001; Gregory *et al.*, 2002; Forest *et al.*, 2002). Existing general circulation models (GCMs) that couple atmosphere-ocean-land components also differ significantly in both climate sensitivity and rate of heat uptake (IPCC, 2001; Raper *et al.*, 2002; Sokolov *et al.*, 2003). An important source of these differences among models is the lack of commonly accepted procedures for accurately handling sub-grid-scale processes, leading to a diversity of parameterizations of these processes.

For example, differences in the representation of cloud processes are a main source of differences in climate sensitivity among models (Cess *et al.*, 1989; Colman, 2003). The heat uptake by the deep ocean also depends on the representation of small-scale processes (Stone, 2004). For example, Dalan *et al.* (2005) showed a strong dependency of the rate of oceanic heat uptake on the value of the diapycnal diffusion coefficient. At the same time Meehl *et al.* (2004) found that, if coupled to different atmospheric models, the ocean component of coupled atmosphere-ocean-land general circulation models (AOGCMs) takes up heat at different rates. Some atmospheric and ocean processes occur on such small scales that, even using the world's fastest computers, global climate models are not able to resolve, and thus climate studies must continue to rely on conventional parameterizations, or "super-parameterizations" (*e.g.*, Randall *et al.*, 2003). It is unlikely that these dynamical and other uncertainties will be substantially reduced within the next decade or more, when important policy choices must nevertheless be made.

Further complicating the analysis task is the century-scale nature of the issue, including the difficulty of projecting anthropogenic emissions of greenhouse gases and aerosols, and possible land-use change, over such a long horizon. Efforts to project population, economic development and technological evolution over many decades necessarily involve great uncertainties. Moreover, these human systems are subject to feedbacks from any future climate change itself, through climatic effects on agriculture and fisheries, effects of sea level rise on coastal regions, and other impacts.

These difficulties make it clear that there is no single best climate model, best set of key climate parameters or best emissions scenario for projecting climate change or assessing policy proposals. Indeed, this characteristic of the climate change issue has led to calls for intensified efforts to quantify the uncertainties (Moss & Schneider, 2000; Reilly *et al.*, 2001). The Intergovernmental Panel on Climate Change (IPCC) made a start toward this goal in their

Third Assessment Report (Allen *et al*., 2001), but their projections for 2100 still included no probabilities or confidence intervals. Much greater attention is being given to this issue in the preparation of the IPCC Fourth Assessment Report. Even with much greater computational power than is available today, however, it will not be possible to fully explore uncertainties in the underlying processes or even to assess proposed emissions control policies using fully complex state-of-the-art AOGCMs. Therefore such studies are usually carried out with models of intermediate complexity (Claussen *et al*., 2002). Recent model intercomparisons have shown that in many cases changes in climate predicted by models of intermediate complexity are very similar to those obtained in the simulations with AOGCMs (Gregory *et al*., 2005; Stouffer *et al*., 2005).

The philosophical framework for a fully-coupled probabilistic approach to the climate problem, and the initial (Version 1) of the MIT Integrated Global System Model (IGSM) designed to implement this framework, was described by Prinn *et al*. (1999). The climate system component of the IGSM was designed to provide the flexibility and computational speed required to handle multiple policy studies and uncertainty analysis while representing to the best degree possible the physics, chemistry and biology of the more computationally intensive AOGCMs. Also, within the IGSM the earth system components are linked to a model of human interactions. The nature of the analysis that such a facility can provide is illustrated by its use to analyze key aspects of the climate issue. For example, the IGSM has been applied to the quantification of uncertainties in future climate. Specifically, Forest *et al*. (2002) used the climate component of the IGSM (Sokolov & Stone, 1998; Prinn *et al*., 1999) to produce probability distributions for the climate sensitivity, the rate of heat uptake by the deep oceans, and the net forcing due to aerosols by comparing observed temperature changes over the 20th century with results of the simulations in which these model parameters were varied. This work was then combined with an analysis of uncertainty in emissions to 2100 (Webster *et al*., 2002) to produce studies of the overall dimensions of the climate threat and the effects of a particular (550 ppm CO_2) stabilization policy (Webster *et al*., 2003). Other examples include the application of the integrated system to analysis of policy goals and measures (*e.g.*, Reilly *et al*., 1999, 2002; Sarofim *et al*., 2004), and to the study of the interaction between greenhouse gas mitigation measures and urban air pollution policy (*e.g.*, Prinn *et al*., 2005).

Each of the IGSM components is being continually improved and extended, and in this paper we describe Version 2, which is the state of the system as of mid-2005. The general thrust of work to improve on the earlier version has been to add climatic, urban air chemistry and economic detail to the existing framework, improving its capability as a facility for integrated assessment of global climate change and urban air pollution. Discussion of the model components is given in Section 2. Section 3 provides a comparison of results between the earlier version of the IGSM system and the current IGSM2, with a special focus on those components concerned with emissions projections and the natural climate system response. Section 4 summarizes ongoing efforts to further improve this research and analysis facility.

2. MODEL COMPONENTS

As depicted in **Figure 1**, the IGSM Version 2 includes sub-models of the relevant aspects of the natural earth system coupled to a model of the human component as it interacts with climate processes. A description of the system components used in Version 1, along with a sensitivity test of key aspects of its behavior, are reported in Prinn *et al.* (1999), and additional characteristics of particular components are described in Babiker *et al.* (2001), Mayer *et al.* (2000), Kamenkovich *et al.* (2002), and other Joint Program Reports, Technical Notes and journal publications.

The major model components of the IGSM2 are shown in Figure 1:

- A model of human activity and emissions (the Emission Prediction and Policy Analysis or EPPA model),
- An atmospheric dynamics, physics and chemistry model, which includes a sub-model of urban chemistry,
- An ocean model with carbon cycle and sea-ice sub-models,
- A linked set of coupled land models, the Terrestrial Ecosystem Model (TEM), a now more fully integrated Natural Emissions Model (NEM), and the Community Land Model (CLM), that encompass the global, terrestrial water and energy budgets and terrestrial ecosystem processes.
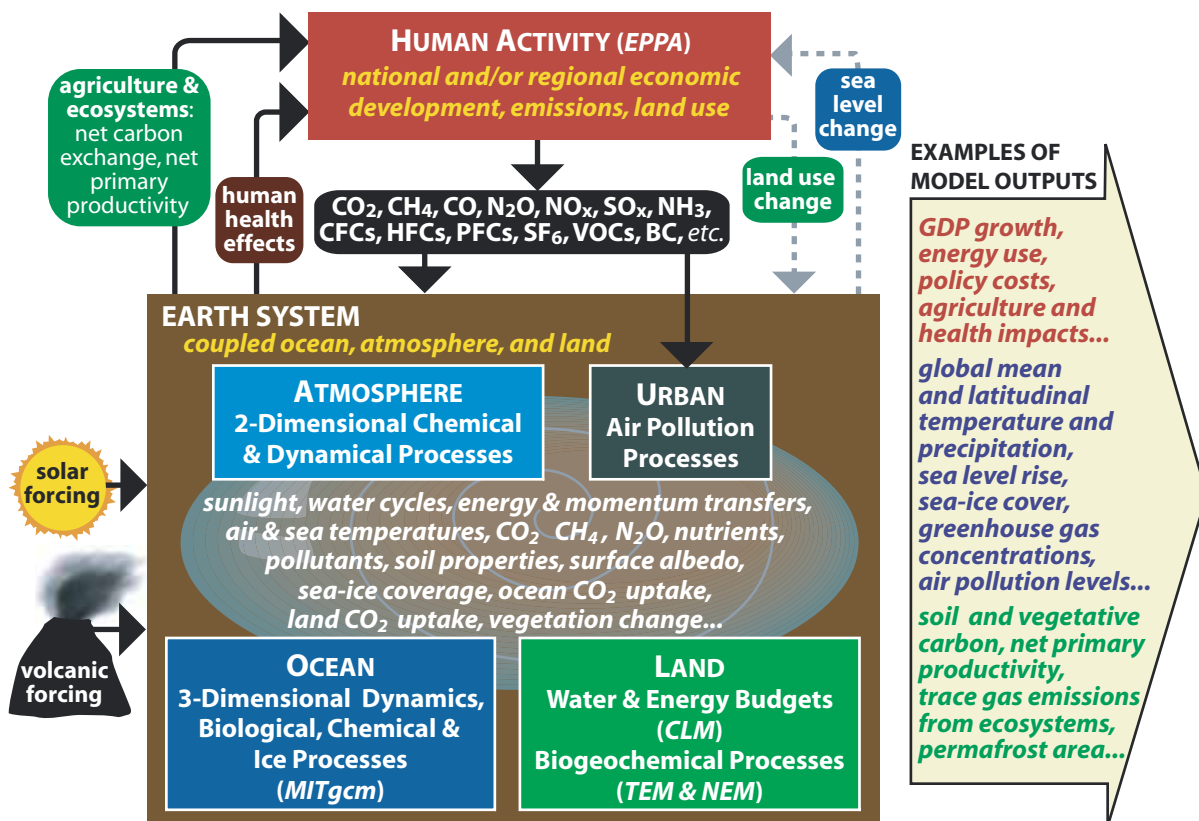
Figure 1. Schematic of the MIT Integrated Global System Model Version 2 (IGSM2).

3

The earth system depicted in Figure 1 represents a fully coupled system that allows simulation of critical feedbacks among its components. Time-steps used in the various sub-models range from 10 minutes for atmospheric dynamics, to 1 month for TEM, to 5 years for the EPPA model, reflecting differences in the characteristic time-scales of different processes simulated by the IGSM. The major model components of the IGSM2 and recent developments in their capabilities and linkages are summarized below.

2.1 Human Activity and Emissions

The MIT Emissions Predictions and Policy Analysis (EPPA) model is a recursive-dynamic multi-regional computable general equilibrium (CGE) model of the world economy. It is built on the GTAP dataset (Dimaranan & McDougall, 2002) augmented by data for the emissions of greenhouse gases, aerosols and other species that are relevant for greenhouse gas and pollution chemistry. The current EPPA version specifically projects economic variables (GDP, energy use, sectoral output, consumption, *etc*.) and emissions of greenhouse gases (CO_2, CH_4, N_2O, HFCs, PFCs and SF_6) and other air pollutants (CO, VOC, NO_x, SO_2, NH_3, black carbon, and organic carbon) from combustion of carbon-based fuels, industrial processes, waste handling, and agricultural activities. Special provision is made for analysis of uncertainty in key human influences, such as the growth of population and economic activity, and the pace and direction of technical change. The model formulation supports analysis of a variety of emissions control policies, providing estimates of the magnitude and distribution among nations of their costs, and clarifying the ways that changes are mediated through international trade.

The version of EPPA (EPPA4) used in IGSM2 is a significant advance compared to the earlier version (EPPA3) described by Babiker *et al.* (2001). The most important advance in terms of earth system modeling is a more complete treatment of technology and material flows. This has required the development and expansion of supplemental tables on physical flows and balances that correspond to economic flows, and developing a correspondence between bottom-up technological detail and National Income and Product Account (NIPA) data that are the basis of any CGE model. Many of these features were developed in versions of EPPA subsequent to the version described in Babiker *et al.* (2001). The importance of these supplemental tables is that they provide the material link to the earth system in terms of physical emissions and land use, and provide the ability to examine energy efficiency in physical units, for example, of electric generation technologies or vehicle fleets, that can be compared with engineering data. EPPA4 brings all of these advances together, and the cumulative effect of these improvements and additions is to provide consistency between economic and key physical flows critical for earth system modeling. Details of Version 4 are provided by Paltsev *et al.* (2005a).

Further highlights of the improvements incorporated in this version include the following. First, compared with the previous version of the model, EPPA4 includes greater geographic disaggregation, shown in **Table 1**. The number of separate regions was increased from twelve to

Table 1. Countries and Regions in the EPPA Model.

Regions in Earlier Versions	Regions in EPPA4	
Annex B		
United States (USA)	United States (USA)	
European Union (EEC)	European Union[a] (EUR)	***Europe Detail for Special Studies***
Eastern Europe (EET)	Eastern Europe[b] (EET)	Great Britain
Japan (JPN)	Japan (JPN)	Finland
Former Soviet Union (FSU)	Former Soviet Union[c] (FSU)	France
Other OECD (OOE)	Australia & New Zealand (ANZ)	Germany
	Canada (CAN)	Hungary
		Italy
Non-Annex B		Netherlands
China (CHN)	China (CHN)	Poland
India (IND)	India (IND)	Spain
Dynamic Asian Economies (DAE)	Higher Income East Asia[d] (ASI)	Sweden
Energy Exporting LDCs (EEX)	Middle East (MES)	EFTA (Switzerland Norway, Iceland)
Brazil (BRA)	Indonesia (IDZ)	Other
Rest of the World (ROW)	Mexico (MEX)	
	Central & South America (LAM)	
	Africa (AFR)	
	Rest of World[e] (ROW)	

[a] The European Union (EU-15) plus countries of the European Free Trade Area (Norway, Switzerland, Iceland)

[b] Hungary, Poland, Bulgaria, Czech Republic, Romania, Slovakia, Slovenia

[c] Russia and Ukraine, Latvia, Lithuania and Estonia (which are included in Annex B) and Azerbaijan, Armenia, Belarus, Georgia, Kyrgyzstan, Kazakhstan, Moldova, Tajikistan, Turkmenistan, and Uzbekistan (which are not)

[d] South Korea, Malaysia, Philippines, Singapore, Taiwan, Thailand

[e] All countries not included elsewhere: Turkey, and mostly Asian countries

sixteen. Canada is now separated from Australia/New Zealand and Mexico is separately identified, a change that will allow a much improved analysis of North America. Developing country groupings have been redefined to more clearly identify the major energy exporting regions such as the Middle East and Indonesia. Also, other changes have been made to create geographically contiguous groups such as Africa and Latin America to better facilitate linkage with other components of the IGSM (such as the land system and the urban air pollution components) that require spatial information.[1] EPPA4 also provides the flexibility to create more finely resolved versions of the model for special studies. One example of this capacity is the disaggregation of the EU-25 (European Union plus Eastern Europe in the sixteen region breakdown) into a set of ten individual countries, and an aggregate that includes the remaining EU-25 countries**.**

Second, as shown in **Table 2** the level of sectoral detail has been expanded over the EPPA version documented by Babiker *et al.* (2001). Services have been separately identified and, of great importance for emissions analysis, the transport sector has been disaggregated. The elaboration of transportation appears in two places in the table: transport was disaggregated from Other Industries and Services in the production sectors, and an activity representing the provision of own-transport (*i.e.*, the private automobile) was added to the Household Sector (Paltsev *et al.*,

---

[1] One further elaboration is planned, but thus far delayed by data gaps, and that is to break out Russia and Ukraine as a separate region, with the remainder of the Former Soviet Union aggregated into Rest of World.

Table 2. Sectoral Breakdown and Resource Factors in the EPPA Model.

Sectors in Earlier Versions	Sectors in EPPA4	
Non-Energy		**Production Sectors**
		Agriculture for Special Studies
Agriculture	Agriculture	Crops
Energy Intensive	Energy Intensive	Livestock
Other Industries & Services	Transportation	Forestry
	Other Industry	
	Services	
Energy		
Electricity *(detail not shown here)*	Electricity	***Electric Generation Technology***
Crude Oil	Conventional Crude Oil	Coal
Oil from Shale	Oil from Shale	Gas
Refined Oil	Liquid Fuel from Biomass	Refined Oil
Coal	Refined Oil	Hydro
Natural Gas	Coal	Nuclear
Gas from Coal	Natural Gas	NGCC[a]
	Gas from Coal	NGCC-CCS[b]
		IGCC-CCS[c]
		Wind & Solar
Household		Biomass
Household Consumption	Own-Supplied Transport	
	Purchased Transport	
	Other Goods & Services	

	Primary Input Factors in EPPA 4	
	For Each Region	***For Energy Resource Sectors***
	Capital	Crude Oil
	Labor	Shale Oil
	Land	Natural Gas
		Coal
		Hydro
		Nuclear
		Wind & Solar

[a] Natural Gas Combined Cycle
[b] Natural Gas Combined Cycle with Carbon Capture and Sequestration
[c] Integrated Gas Combined Cycle with Carbon Capture and Sequestration

2004; Paltsev *et al*., 2005b). This formulation of the Household Sector thus identifies both automobile emissions and those associated with purchased transport by households (air, bus and train). Emissions related to freight and passenger transportation not purchased by households are also part of the commercial transport sector, and this transport service is supplied as an intermediate good to other sectors. This further disaggregation allows a more careful study of the potential growth of transportation over time, and of the implications for an economy's energy and carbon intensity. The private automobile accounts for roughly one-quarter of US CO_2 emissions and somewhat less in other OECD nations, and it represents a growing fraction of emissions in most developing countries.

As shown in Table 2, for special studies the agriculture sector can be disaggregated into Crops, Livestock and Forestry, with an explicit treatment of land used in each sector. This new facility is useful for analysis of emissions from agriculture, and of the effects of climate change

and air pollution on crops and forestry, and can incorporate results (feedbacks) from TEM that describe changes in crop and forest productivity (Reilly *et al.*, 2004).

Third, the specification of energy supply technologies, also shown in Table 2, has been expanded from that in earlier versions. The provision of liquid fuel from biomass has been added as a technology that competes with the agricultural sector for land resources. The most significant extensions, however, have been made in the electric power sector. Generation technologies in earlier versions of the EPPA structure (not detailed in the table) included fossil, hydro, nuclear, and an undifferentiated carbon-free electric or renewable source (Babiker *et al.*, 2001). In EPPA4 much greater specificity is provided. Two explicit renewable alternatives are included: a wind and solar source and biomass-based generation (again, competing with agriculture for land inputs). Also, several technologies have been incorporated to support assessment of carbon capture and storage (McFarland *et al.*, 2004). Capture and storage (CCS) options based on both natural gas combined cycle (NGCC-CCS) and integrated coal gasification combined cycle generation (IGCC-CCS) are included, and to represent the proper competitive conditions for these CCS technologies an NGCC technology without capture has been included as well.

Fourth, the economic and non-CO_2 emissions data have been updated and greatly improved. These changes include the following:

- Incorporation of an updated GTAP 5 data set (Dimaranan & McDougall, 2002).
- Updating of the demographic data and future projections (United Nations, 2000).
- General revision of projected economic growth and inventories of non-CO_2 greenhouse gases and urban pollutants.

The EPPA model has also been substantially revised to support more complex policy descriptions, particularly measures that differ among countries and among sectors and the instruments applied, and to facilitate the processing of model results. Highlights of these improvements include the following:

- Logic has been added to facilitate the analysis of greenhouse gas control policies that apply differential measures across sectors and among gases.
- Methods have been implemented for analyzing the economic effects of air pollution damage and other climate-related effects within EPPA's general equilibrium framework (*e.g.*, Yang *et al.*, 2005).
- Provision has been made for simulation of international agreements that apply to various subgroups of countries, and differentiate by gas or sector.

To facilitate the analysis of EPPA results, output files have been reconfigured and flexible graphing software has been developed.

Finally, the key linkage between EPPA's emissions output and the earth system model (Figure 1) is the emissions postprocessor. This postprocessor is based on the work of Mayer *et al.* (2000). It has been updated to reflect the increased spatial resolution of the earth system

model and the sixteen regions of the EPPA4 model, and uses an updated population map based on the Gridded Population of the World (GPW), Version 2 (CIESIN, 2000). We further assume that the atmospheric carbon source in biogenic emissions of methane (CH_4) and carbon monoxide (CO) from human activity projected by EPPA is balanced by a carbon (CO_2) sink to account for the fact that these emissions are from annually regrown crops. Projections of the Montreal Protocol (Ozone Layer Protection) gases and aerosol emission data for the 1980s were also updated with data from the Global Emissions Inventory Activity (GEIA, 2005).

2.2 Atmospheric Dynamics and Physics

The MIT two-dimensional (2D) atmospheric dynamics and physics model (Sokolov & Stone, 1998) is a zonally-averaged statistical dynamical model that explicitly solves the primitive equations for the zonal mean state of the atmosphere and includes parameterizations of heat, moisture, and momentum transports by large-scale eddies based on baroclinic wave theory (Stone & Yao, 1987, 1990). The model's numerics and parameterizations of physical processes, including clouds, convection, precipitation, radiation, boundary layer processes, and surface fluxes, build upon those of the Goddard Institute for Space Studies (GISS) GCM (Hansen *et al.*, 1983). The radiation code includes all significant greenhouse gases (H_2O, CO_2, CH_4, N_2O, CFCs and O_3) and eleven types of aerosols. The model's horizontal and vertical resolutions are variable, but in the standard version of IGSM2 it has 4° resolution in latitude and eleven levels in the vertical. The earlier IGSM version had a resolution of 7.8° in latitude and nine vertical levels.

The MIT 2D atmospheric dynamics and physics model allows up to four different types of surface in the same grid cell (ice free ocean, sea-ice, land, and land-ice). The surface characteristics (*e.g.*, temperature, soil moisture, albedo) as well as turbulent and radiative fluxes are calculated separately for each kind of surface while the atmosphere above is assumed to be well mixed horizontally in each latitudinal band. The area weighted fluxes from different surface types are used to calculate the change of temperature, humidity, and wind speed in the atmosphere. Fluxes of sensible heat and latent heat are calculated in the atmospheric model by bulk formulas with turbulent exchange coefficients dependent on the Richardson number. The atmosphere's turbulence parameterization is also used in the calculation of the flux derivatives with respect to surface temperature. To account for partial adjustment of near surface air temperature to changes in fluxes the derivatives are calculated under the assumption that the exchange coefficients are fixed. A more detailed discussion of technical issues involved in the calculations of these fluxes and their derivatives is given in Kamenkovich *et al.* (2002). The atmospheric model's climate sensitivity can be changed by varying the cloud feedback (Sokolov & Stone, 1998; Sokolov, 2005).

2.3 Urban and Global Atmospheric Chemistry

To calculate atmospheric composition, the model of atmospheric chemistry includes an analysis of the climate-relevant reactive gases and aerosols at urban scales, coupled to a model of

the processing of exported pollutants from urban areas (plus the emissions from non-urban areas) at the regional to global scale. For calculation of the atmospheric composition in non-urban areas, the above atmospheric dynamics and physics model is linked to a detailed 2D zonal-mean model of atmospheric chemistry. The atmospheric chemical reactions are thus simulated in two separate modules, one for the 2D model grids and one for the sub-grid-scale urban chemistry.

2.3.1 Urban Air Chemistry

The analysis of the atmospheric chemistry of key substances as they are emitted into polluted urban areas is an important addition to the integrated system since the version described in Prinn *et al.* (1999). Urban airshed conditions need to be resolved at varying levels of pollution. The urban air chemistry model must also provide detailed information about particulates and their precursors important to air chemistry and human health, and of the effects of local topography and structure of urban development on the level of containment and thus intensity of air pollution events. This is an important consideration since air pollutant levels are dependent on projected emissions per unit area, not just total urban emissions.

The urban atmospheric chemistry model was first introduced as an additional component to the original global model (Prinn *et al.*, 1999) in IGSM1 (Calbo *et al.*, 1998; Mayer *et al.*, 2000; Prinn *et al.*, 2005). This initial urban chemistry module was derived by fitting multiple runs of the detailed 3D California Institute of Technology (CIT) Urban Airshed Model. Similar to IGSM1, the urban model in IGSM2 (Prinn & Cohen, 2005) uses the probabilistic collocation method to express outputs from a detailed 3D model in terms of model inputs using polynomial chaos expansions (Tatang *et al.*, 1997). However, the new urban 3D model chosen is the state-of-the-art Comprehensive Air Quality Model with Extensions (CAMx, described by Byun *et al.,* 2005). Also the range of inputs is expanded to incorporate wider ranges of emitted pollutants, intra-urban topographies (a flexible feature in CAMx), spatial and temporal distributions of emissions, and future urban development scenarios. Similarly the range of outputs is extended to include several new measures of pollutants and pollutant levels relevant to human health. The required probability distribution functions for the emission and climate inputs utilize the results from the existing large ensembles of IGSM runs for future emissions (Webster *et al.*, 2002) and future climates (Webster *et al.*, 2003). Instead of the three urban types in IGSM1 (low, medium, high pollution levels), IGSM2 incorporates separate polynomial parameterizations for multiple emission intensities and for "representative cities" in each EPPA region for each 4° latitude band. The outputs over time from each representative city then apply to the total urban population in the relevant EPPA country or region. These various significant improvements enable us to better account for the full range of urban topographies, emission patterns, climates, and degrees of economic development, in our studies of pollutant impacts on human health, downwind ecosystems and global atmospheric composition and climate.

2.3.2 Global Atmospheric Chemistry

The 2D zonal mean model that is used to calculate atmospheric composition is a finite difference model in latitude-pressure coordinates, and the continuity equations for trace constituents are solved in mass conservative or flux form (Wang *et al.*, 1998). The model includes 33 chemical species. The continuity equations for $CFCl_3$, CF_2Cl_2, N_2O, O_3, CO, CO_2, NO, NO_2, N_2O_5, HNO_3, CH_4, CH_2O, SO_2, H_2SO_4, HFC, PFC, SF_6, black carbon aerosol, and organic carbon aerosol include convergences due to transport, parameterized north-south eddy transport, convective transports, local true production or loss due to surface emission or deposition, and atmospheric chemical reactions. In contrast to these gases and aerosols, the very reactive atoms (*e.g*., O), free radicals (*e.g*., OH), or molecules (*e.g*., H_2O_2) are assumed to be unaffected by transport because of their very short lifetimes; only chemical production and/or loss (in the gaseous or aqueous phase) is considered in the predictions of their atmospheric abundances.

There are 41 gas-phase and twelve heterogeneous reactions in the background chemistry module applied to the 2D model grid. The scavenging of carbonaceous and sulfate aerosol species by precipitation is also included using a method based on a detailed 3D climate-aerosol-chemistry model (Wang, 2004). Water vapor and air (N_2 and O_2) mass densities are computed using full continuity equations as a part of the atmospheric dynamics and physics model to which the chemical model is coupled. The climate model also provides wind speeds, temperatures, solar radiation fluxes and precipitation, which are used in both the global and urban chemistry formulations.

2.4 Ocean Component

A zonally (longitudinally) averaged mixed-layer model with 7.8° latitudinal resolution was used as an ocean component in the IGSM1 (Prinn *et al.*, 1999). In the IGSM2 it has been replaced by either a 2D (latitude-longitude) mixed-layer anomaly-diffusing ocean model (IGSM2.2) or a fully 3D ocean GCM (IGSM2.3). The version used in a particular case is selected depending on the nature of the application.

2.4.1 The 2D Ocean Model

The IGSM2.2 has a mixed-layer anomaly-diffusing ocean model with a horizontal resolution of 4° in latitude and 5° in longitude. Mixed-layer depth is prescribed based on observations as a function of time and location (Hansen *et al.*, 1983). Vertical diffusion into the deep ocean is handled similar to IGSM1, but now a diffusion coefficient varies zonally as well as meridionally.

The coupling between the atmospheric and oceanic models takes place every hour. The heat flux (F_H) at the longitude-latitude point (*i*, *j*) is calculated as:

$$F_H(i, j) = F_{HZ}(j) + \frac{\partial F_{HZ}}{\partial T}(j)(Ts(i, j) - Tsz(j)) , \tag{1}$$

where

$F_{HZ}(j)$ and $\partial F_{HZ}/\partial T (j)$ = zonally averaged heat flux and its derivative with respect to surface temperature, and

$Ts(i,j)$ and $Tsz(j)$ = surface temperature and its zonal mean.

Similar to IGSM1, the mixed-layer model also includes specified vertically-integrated horizontal heat transport by the deep oceans, a so-called "Q-flux," but now allowing zonal as well as meridional transport. This flux has been calculated from a simulation in which sea surface temperature and sea-ice distribution were relaxed toward their present-day climatology with relaxation a coefficient of 300 Wm^{-2}/K, corresponding to an e-folding time-scale of about 15 days for the 100 m deep mixed-layer. Use of a 2D (longitude-latitude) mixed-layer ocean model (IGSM2.2) instead of a zonally-averaged model (IGSM1) has allowed a better simulation of both the present day sea-ice distribution and sea-ice change in response to an increasing forcing.

A thermodynamic ice model is used for representing sea ice. The model has two layers and computes ice concentration (the percentage of area covered by ice) and ice thickness. The IGSM2.2 includes the same ocean carbon model (Holian *et al.*, 2001) as the IGSM1.

The IGSM's 2D atmospheric model coupled to a Q-flux mixed-layer/diffusive ocean model of the above type has been shown, with an appropriate choice of the model's cloud feedback and effective diffusion coefficient, to reproduce the transient surface warming and sea level rise due to thermal expansion of the ocean as calculated in various coupled AOGCMs for 120-150 year time-scales (Sokolov & Stone, 1998; Sokolov *et al.*, 2003). This Q-flux model cannot, however, represent feedbacks associated with fundamental changes in the ocean circulation. In applications that need to take into account possible interactions between atmosphere and ocean circulation, the diffusive ocean model is therefore replaced by a fully 3D ocean GCM in the IGSM2.3.

2.4.2 The 3D Ocean General Circulation Model

The 3D ocean component, depicted in **Figure 2**, is a major advance in the capabilities of the IGSM. The IGSM1 atmospheric model (with lower resolution than in the IGSM2) had previously been coupled to the MOM2 ocean GCM for studies of ocean response to climate change (Kamenkovich *et al.*, 2002, 2003; Dalan *et al.*, 2005a,b; Huang *et al.*, 2003a,b). This version was also used in a number of model intercomparison studies (Gregory *et al.*, 2005; Petoukhov *et al.*, 2005; Stouffer *et al.*, 2005). However, as detailed by Dutkiewicz *et al.* (2005) the 3D ocean-seaice-carbon cycle component of the IGSM2.3 is now based on the state-of-the-art 3D MIT ocean general circulation model (Marshall *et al.*, 1997a,b). As configured for the IGSM2.3, the MIT ocean model has realistic bathymetry, and 4° by 4° resolution in the horizontal with fifteen layers in the vertical. Mesoscale eddies, which are not captured in this coarse resolution, are represented by the Gent & McWilliams (1990) parameterization. Embedded in the ocean model is a thermodynamic sea-ice model based on the 3-level model of Winton (2000) and the LANL CICE model (Bitz & Lipscome, 1999).
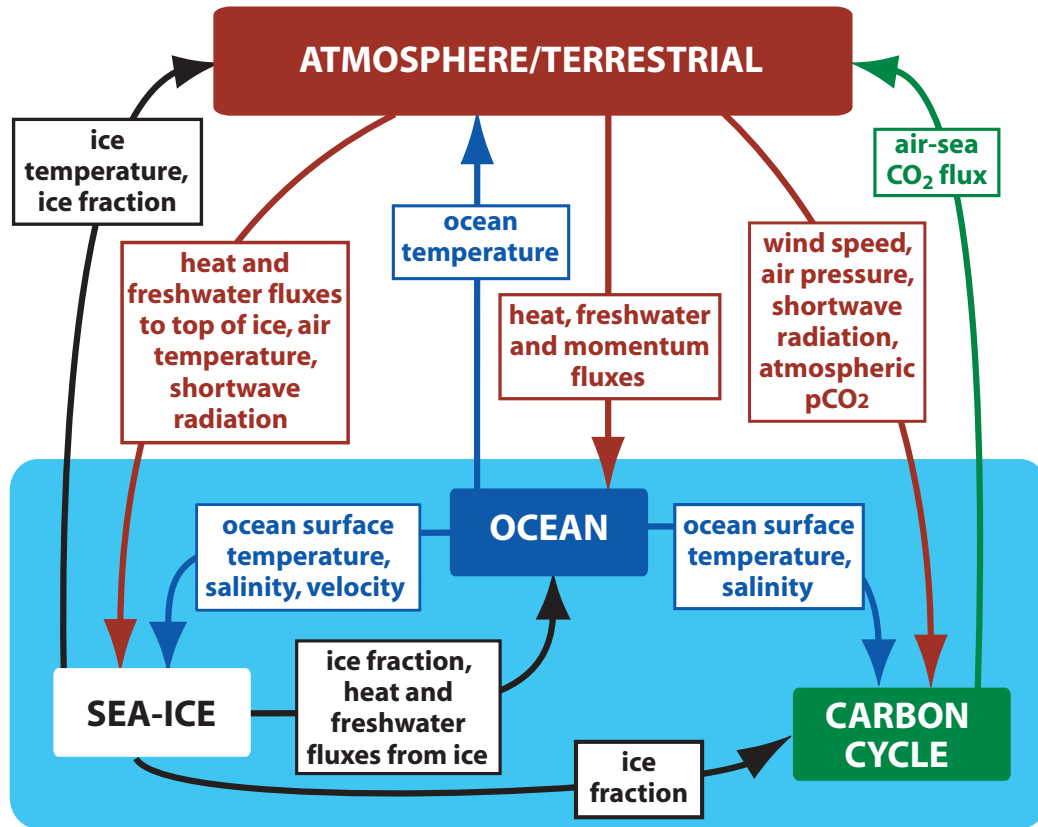
Figure 2. Schematic of the ocean model component of the IGSM2.

The ocean model has a biogeochemical component with explicit representation of the cycling of carbon, phosphorus, and alkalinity. The physical ocean model velocities and diffusion are used to redistribute these tracers. Air-sea exchange of carbon dioxide follows Wannikof (1992), and carbonate chemistry is calculated following Najjar & Orr (1998), Millero (1995), and the DOE Handbook (1994). We also parameterize the export of organic carbon from the surface waters: biological productivity is modeled as a function of available nutrient (phosphate) and light (see Dutkiewicz *et al*., 2005), similar to Parekh *et al*., 2005. There is also a representation of the calcium carbonate cycle following the parameterization of Yamanaka & Tajika (1996).

The coupling between the atmospheric and oceanic sub-models takes place once a day. The atmospheric model calculates 24-hour means of surface heat, freshwater and momentum fluxes and passes these to the ocean model. After receiving these fluxes from the atmosphere, the ocean and sea-ice sub-models are integrated for 24 hours (two ocean tracer time-steps). At the end of this period, sea surface temperatures, surface ice temperatures, and sea-ice coverage are passed back to the atmospheric sub-model.

The atmospheric sub-model provides heat and fresh-water fluxes separately over the open ocean and over sea ice, as well as their derivatives with respect to surface temperature. Total heat and fresh-water fluxes for the oceanic sub-model can therefore vary by longitude as a function of ocean sea surface temperature, *i.e*., warmer ocean locations undergo greater evaporation and

receive less downward heat flux (similar to the procedure represented in Equation 1). Wind stresses from the atmospheric sub-model are weaker than observations, especially in the Southern Ocean. The oceanic sub-model therefore uses the technique of anomaly coupling: the mean wind stresses, including zonal variations, are taken from the climatology of Trenberth *et al.* (1989), while the anomalies are taken from the atmospheric sub-model. The oceanic sub-model requires adjustments to the atmospheric heat and freshwater fluxes in order to replicate the ocean sea surface temperature and salinity of the later part of the 20th century. These adjustments are calculated as part of the ocean sub-model spin-up, and then are held fixed over the simulation of 1860 onward. In this 3D configuration, the ocean-carbon-atmospheric component must be spun-up for several thousand years to reach a pre-industrial (1860) steady state. More details of the ocean-carbon-seaice sub-model and its coupling to the atmosphere are provided by Dutkiewicz *et al.* (2005).

2.5 Land and Vegetation Processes

The component of the IGSM2 that represents the global land processes is a dynamically linked set of terrestrial biogeophysical (*i.e.*, water and energy budgets) and biogeochemical (*i.e.*, carbon and nitrogen) sub-models. The significantly revised treatment of land systems in the IGSM2 guarantees conservation of water and energy between these sub-models, which was not assured in the IGSM1 treatment. The new representation of land processes is also designed to be flexibly run either with the meridional resolution (4º) of the IGSM2 zonally-averaged atmospheric model, or with a latitude-longitude grid (*e.g*., 4º by 4º). The coarser resolution compared with the 0.5º by 0.5º resolution of the TEM is numerically more efficient than the previous scheme. Further, the use of a mosaic scheme (described below) within each grid retains a realistic treatment of multiple vegetation types without the need for a very fine grid resolution. The new system employs three coupled sub-models to represent the terrestrial water, energy, and ecosystem processes:

- The Community Land Model (CLM) described by Bonan *et al.* (2002) calculates the global, terrestrial water and energy balances.
- The Terrestrial Ecosystems Model (TEM) of the Marine Biological Laboratory (Melillo *et al*., 1993; Xiao *et al.*, 1997, 1998; Felzer *et al*., 2004) simulates carbon CO_2 fluxes and the storage of carbon and nitrogen in vegetation and soils including net primary production and carbon sequestration or loss.
- The Natural Emissions Model (NEM) described by Liu (1996) and Prinn *et al.* (1999), now embedded within TEM, simulates fluxes of CH_4 and N_2O.

Further, in the IGSM2 a Global Land Systems (GLS) framework, shown in **Figure 3**, now combines these biogeophysical (*i.e.*, water and energy budgets) and biogeochemical (*i.e.*, carbon, methane, and nitrous oxide fluxes) calculations into a single, self-consistent framework for the global terrestrial environment. Schlosser & Kicklighter (2005) provide a detailed description of

Biogeophysical and Biogeochemical Pathways in the IGSM Global Land System (GLS)
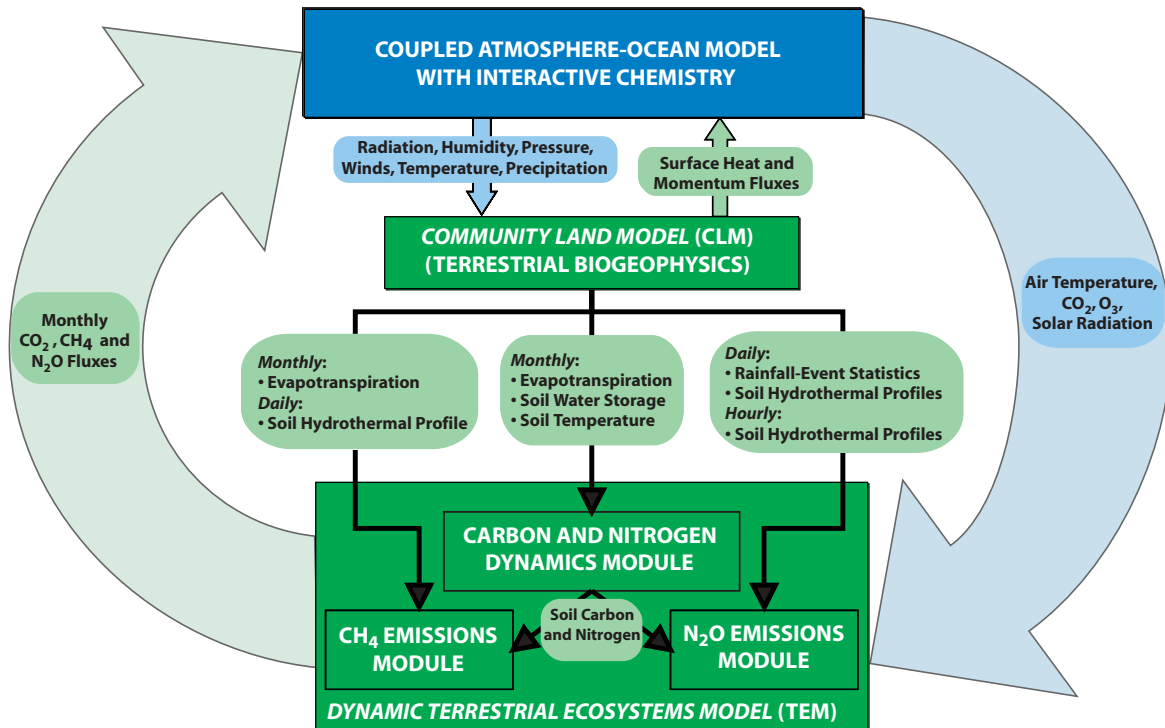
Figure 3. Schematic of coupling between the atmospheric model (which also includes linkages to the air chemistry and ocean models) and the land model components of the IGSM2, also shown are the linkages between the biogeophysical (CLM) and biogeochemical (TEM) subcomponents. All green shaded boxes indicate fluxes/storage that are explicitly calculated/tracked by this Global Land System (GLS). The blue shaded boxes indicate those quantities that are calculated by the atmospheric model of the IGSM2.

the GLS framework, the models employed, and the coupling methodology. The CLM is based upon the Common Land Model (Zeng *et al.*, 2002) derived from a multi-institutional collaboration of land models, and as tested by Dai *et al.* (2003). The CLM is widely used in global-scale land data assimilation research (*e.g.,* Rodell *et al.*, 2004) as well as coupled climate prediction studies (*e.g.,* Dai *et al.*, 2004; Duffy *et al.*, 2003; Govindasamy *et al.*, 2003; Holland, 2003), with well documented characteristics. It provides estimates of soil moisture and temperature profiles, as well as evapotranspiration rates that are required inputs for the TEM and NEM components that are used to estimate fluxes of CO_2, nitrous oxide (N_2O) and CH_4 between terrestrial ecosystems and the atmosphere.

The CLM serves as the interface between these sub-models, and with other major components of the IGSM (Figure 1). All inputs into the GLS framework that require a temporal sampling resolution at the time-step of the atmospheric physics model processes (1 hour) are provided to CLM (as shown in Figure 3); CLM then calculates surface heat and momentum fluxes that are passed back to the atmospheric model. The calculations of these soil/vegetation water and energy fluxes (and corresponding storages and temperatures) are averaged and accumulated as necessary given the time-steps of TEM and NEM.

The major update to the NEM configuration (as compared to IGSM1) is that NEM is now embedded within the TEM infrastructure. As such, the N_2O flux estimates by NEM are directly based on TEM estimates of soil organic carbon. Although the simulated carbon and nitrogen dynamics of NEM are still separated from those in TEM, the embedded NEM now provides a platform for improving the linkages between the two biogeochemistry-models. The more consistent carbon and nitrogen dynamics in IGSM2 supports the development of even better estimates of CO_2, CH_4 and N_2O fluxes in future versions of the IGSM. For example, efforts are already underway to replace the CH_4 module of NEM with the more process-based module of Zhuang *et al.* (2004). Further, the embedded NEM allows simulation of daily CH_4 and N_2O emissions based on monthly estimates of soil organic carbon by TEM combined with the CLM estimates of daily soil temperatures, daily and hourly soil moistures, hourly rainfall intensities and storm durations. Rainfall intensity and storm duration are based on a stochastic Poisson model that is employed by CLM (see Schlosser & Kicklighter, 2005). The GLS framework (Figure 3) also includes the negative influence of ozone on plant productivity (Felzer *et al.*, 2004, 2005).

Incorporation of the vegetation mosaic scheme now means that land cover and climate information used by the embedded NEM and TEM, as well as CLM, are all at the same spatial resolution. The representation of land cover and climate has also been improved from IGSM1 under the GLS framework of the IGSM2. The basic land cover categories used by CLM (Bonan *et al.*, 2002) have been adopted, with a further disaggregation of wetlands into six categories based on the presence or absence of a dominant tree cover and ecological region (*i.e.*, boreal, temperate, tropical). Four floodplain categories have also been added to better support the trace gas flux simulations of TEM and NEM. The modified CLM land categories are denoted as IGSMVEG categories. To allow eventual evaluation of the effects of human activities on terrestrial carbon and nitrogen dynamics, the potential vegetation (*i.e.*, natural vegetation in the absence of human activity) data set of Melillo *et al.* (1993) has been translated into the IGSMVEG categories and the 0.5º by 0.5º data has been aggregated into a mosaic of vegetation types for each 4º zonal band (used by the atmospheric component of IGSM2). The wetlands data set of Matthews & Fung (1987) has also been incorporated into this zonal vegetation mosaic. To estimate CO_2, CH_4 and N_2O fluxes from terrestrial ecosystems, TEM and NEM are run for every vegetation type in the mosaic and the results are area-weighted to obtain aggregate fluxes from each 4º zonal band. As noted above, the GLS uses the zonal climate that is calculated by the 2D atmospheric model and therefore requires no interpolation of the zonal climate to a finer grid. In IGSM1, a baseline climate developed from the Leemans & Cramer (1990) database is used by TEM at a spatial resolution of 0.5º latitude by 0.5º longitude (Xiao *et al.*, 1997) and a similar baseline climate is used by NEM at a spatial resolution of 2.5º latitude by 2.5º longitude (Liu, 1996). The new representation of land cover and climate of the GLS has also been designed such that the terrestrial component of the IGSM has the flexibility to use gridded climate inputs (*e.g.,* 4º latitude by 4º longitude) just as easily as zonal climate inputs (*e.g.*, 4º zonal bands).

3. COMPARISONS AMONG MODEL VERSIONS

Here we carry out a series of computational experiments to explore the differences in behavior of the IGSM in its Version 2 compared to the earlier version. We first discuss revisions that affect the emissions projections and then the implications of changes in the natural science components of the system.

3.1 Comparison of EPPA4 with EPPA3

Economic growth is one of the most important, and uncertain, driver of emissions growth. In EPPA3 (Babiker *et al.*, 2001) the global economy grew 10.7 times from 2000 to 2100, or at 2.4% per year (annual average). Revised demographic projections, including the labor force, and new projections of labor productivity in all regions have resulted in somewhat higher growth in EPPA4 (Paltsev *et al.*, 2005a), with the global economy growing by 12.5 times from 2000 to 2100 or 2.5% per year.

The sensitivity of emissions projections to assumptions about long-term growth are shown in **Figure 4**, which for EPPA4 presents the projected CO_2 emissions with the reference (2.5% average per year), slower (2.0%) and faster (3.0%) economic growth. With the reference GDP growth of 2.5% per year CO_2 emissions in EPPA4 reach 25.7 GtC/yr by 2100, up from the 23.0 GtC/yr projected with the EPPA3 reference GDP growth of 2.4% per year. The nearly 3 GtC/yr increase in emissions is substantial but should be considered in light of the uncertainty in forecasts of economic growth. Further regional and sectoral disaggregation, revisions of autonomous energy efficiency improvement in developing countries, the addition of a broader set of technological options, reevaluation of fossil fuel resources, and other changes as discussed below also affect emissions growth. The non-CO_2 emissions projected by EPPA4 are similarly sensitive to GDP growth but this sensitivity is not shown in Figure 4. A fuller evaluation of the sensitivity of results to GDP growth and other drivers is provided in Webster *et al.* (2002) for EPPA3 and Paltsev *et al.* (2005a) for EPPA4.

Differences among the model versions for the reference values of the non-CO_2 greenhouse gases (GHGs) are also shown in Figure 4. These solutions differ for a number of reasons in addition to the revised GDP growth rates, as detailed in Asaadorian *et al.* (2005). Emissions factors for each sector were revised to be consistent with the new base year (1997) global emissions inventories developed by the US EPA (US EPA, 2001, 2002) and further adjusted to be consistent with inverse calculations for methane from rice (Chen, 2003; Chen & Prinn, 2005). As a result, PFC and NH_3 emissions in 1997 are lower in EPPA4 than in EPPA3, but base year (1997) emissions for other gases were not substantially changed. EPPA4 forecasts for CH_4 are somewhat lower than EPPA3 primarily because of the expected more rapidly falling emissions coefficient over time for methane from fossil fuel production, particularly in Russia.

Nitrous oxide emissions in EPPA4 are somewhat higher than EPPA3 reflecting the higher economic growth, reevaluation of likely future emissions from adipic and nitric acid production,
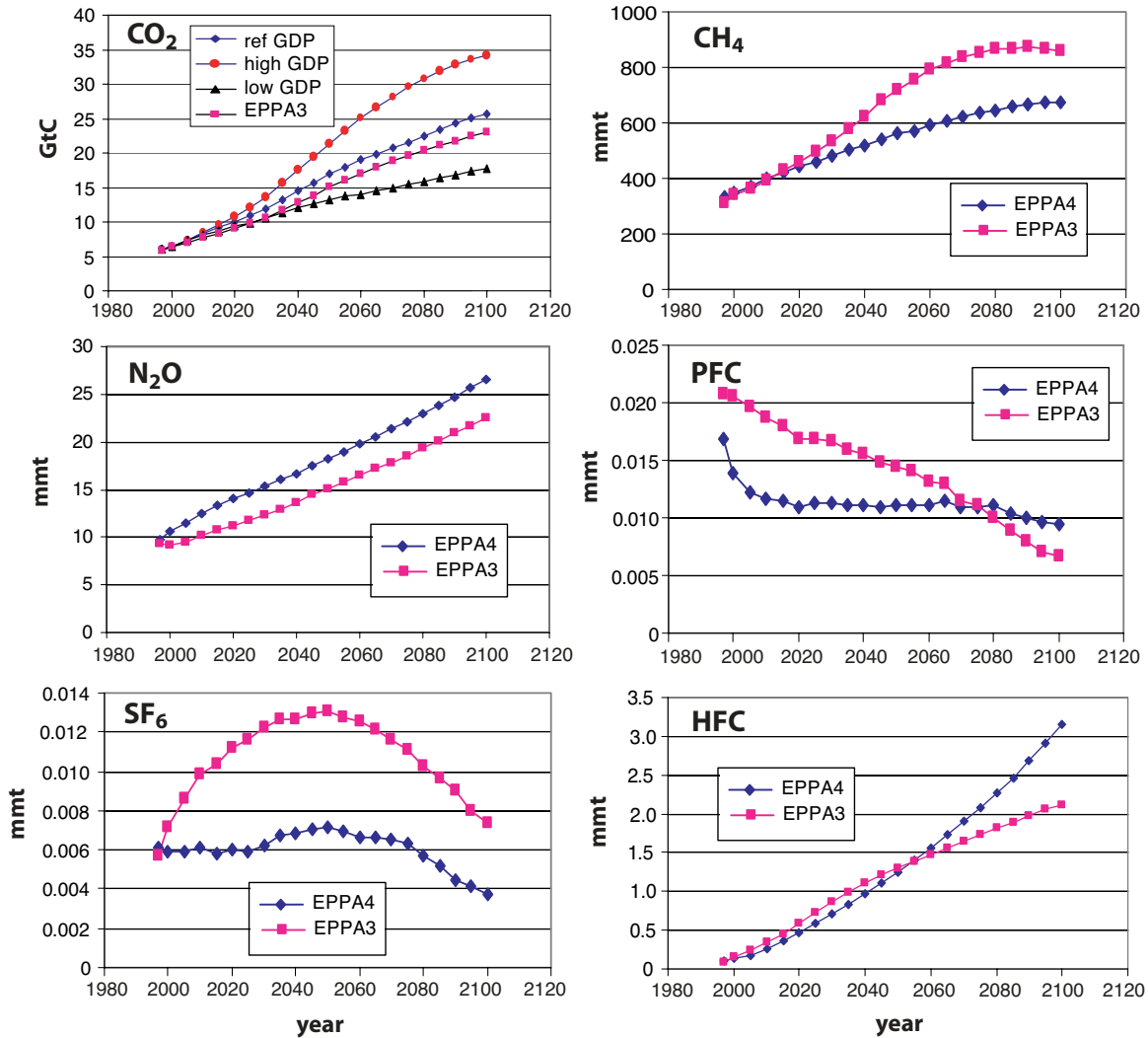
Figure 4. Emissions projections for greenhouse gases.

and revisions to agricultural sources based on new projections of growth of agricultural emitting activities from the International Food Policy Research Center (Rosegrant *et al.* 2002). Significant changes in projections for PFCs, SF_6, and HFCs occurred as a result of further sectoral disaggregation that affects the growth of source sectors for these emissions including the Energy Intensive Industry, Other Industry and Transportation sectors and, for SF_6 in particular, the further disaggregation of the electric sector.

We have sought to define reference projections as the level of emissions if there were no explicit greenhouse gas abatement policies. Now that countries and individual companies have begun to implement mitigation measures in anticipation of future policies such a definition of the reference case may for some regions yield estimates for near-future years that diverge slightly from realized values or other short-term forecasts. This definition of the reference is maintained to allow estimation of the full cost of meeting climate-related commitments. In practice it is not always possible to clearly determine whether reductions have occurred because of anticipated climate policy or for other reasons.

17

The differences between EPPA4 and EPPA3 projections for other substances (gases, aerosols) relevant to atmospheric chemistry and the radiative balance are shown in **Figure 5**. In developing EPPA4 all of the inventories were re-evaluated based on EDGAR 3.2 (Olivier &
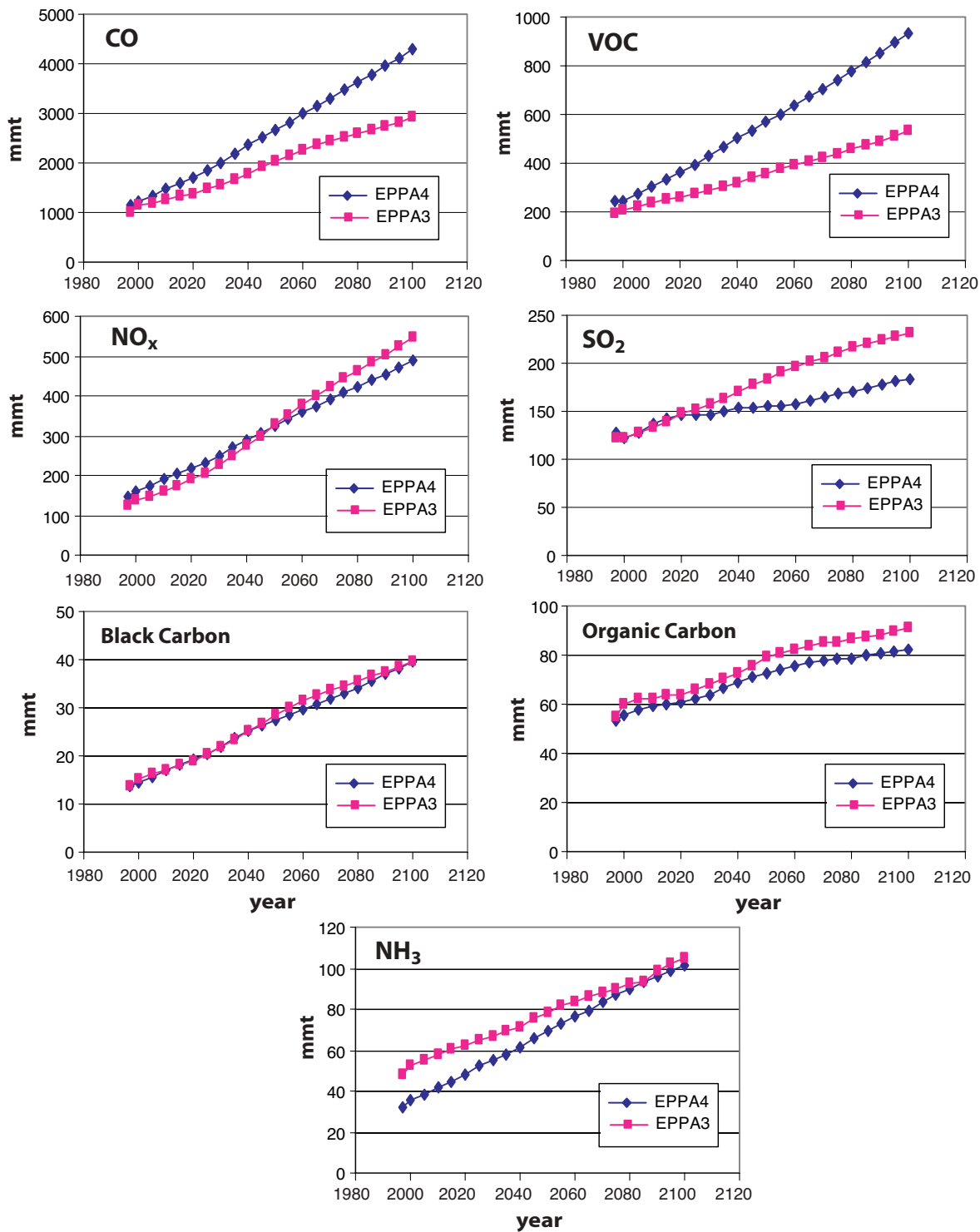
Figure 5. Emissions projections for criteria pollutants.

Berdowski, 2001). Emissions coefficients for different pollutant sources for these were estimated as a function of income per capita in EPPA3. These relationships were re-estimated based on the cross-section benchmark data for 1997 used in EPPA4 (Asadoorian *et al.,* 2005). In addition, to better simulate changes in these coefficients over time the cross-section data were augmented by information on best available practices. In most cases these revisions led to somewhat faster decline with income in the emissions coefficients. A higher GDP implies a more rapidly declining emissions factor.

The large increase in VOC (volatile organic compound) and CO (carbon monoxide) emissions is due to rapid growth of automobile use that is better captured in EPPA4 with the household transportation sector explicitly modeled. The addition of NGCC electric generation technology allows greater penetration of gas in the electric sector in EPPA4 as compared with EPPA3 and this change, along with more rapid decline in the emissions coefficient for SO_2, contributes to lower SO_2 emissions in EPPA4 compared with EPPA3.

These forecasts of criteria pollutants might imply violations of air quality standards in some regions (*e.g.,* US, Europe, Japan), and it can be argued that these air quality standards should be imposed in a reference forecast as an aspect of "business-as-usual." The variety and complexity of regulations, partial coverage of sources, and the fact that policies are often targeted at concentrations rather than emissions means that there is no ready translation of existing policies into specific caps on emissions from sources within countries. Moreover, given the increasing contribution of transboundary pollution sources, a country may find it unable to realistically meet its air pollution goals by limiting emissions of the domestic sources under its control. Our approach is thus to represent the existing "best available" technology rather than assume development of ever-cleaner combustion technology at no cost. Analysis of the impact on ecosystems and urban pollution of lower emissions of these substances is provided by Prinn *et al.* (2005) and Felzer *et al.* (2005).

Changes to EPPA4 were also designed to allow more realistic simulation of the evolution of energy use and economic growth, including greater technological detail and re-evaluation of the pace of energy efficiency improvement as discussed in Section 2.1. A useful summary statistic that captures many of these effects is the change in an economy's energy intensity, which we show for the sixteen EPPA4 regions (top panel) in **Figure 6** and the twelve EPPA3 regions (lower panel). EPPA treats international trade so the model necessarily calculates and reports all currency values at Market Exchange Rates (MER). Cross-country comparisons of these values in the original units (EJ/1997 US$) are not meaningful unless converted to an international currency unit such as Purchasing Power Parity (PPP). Hence, in Figure 6 regional results are each indexed to 1.0 in the base year.

A major consequence of these changes is that some developing countries continue on a path where energy intensity either falls slightly or rises for the first 20 to 40 years. Declining energy intensity is consistent with recent history in the developed countries, but as reviewed in Babiker
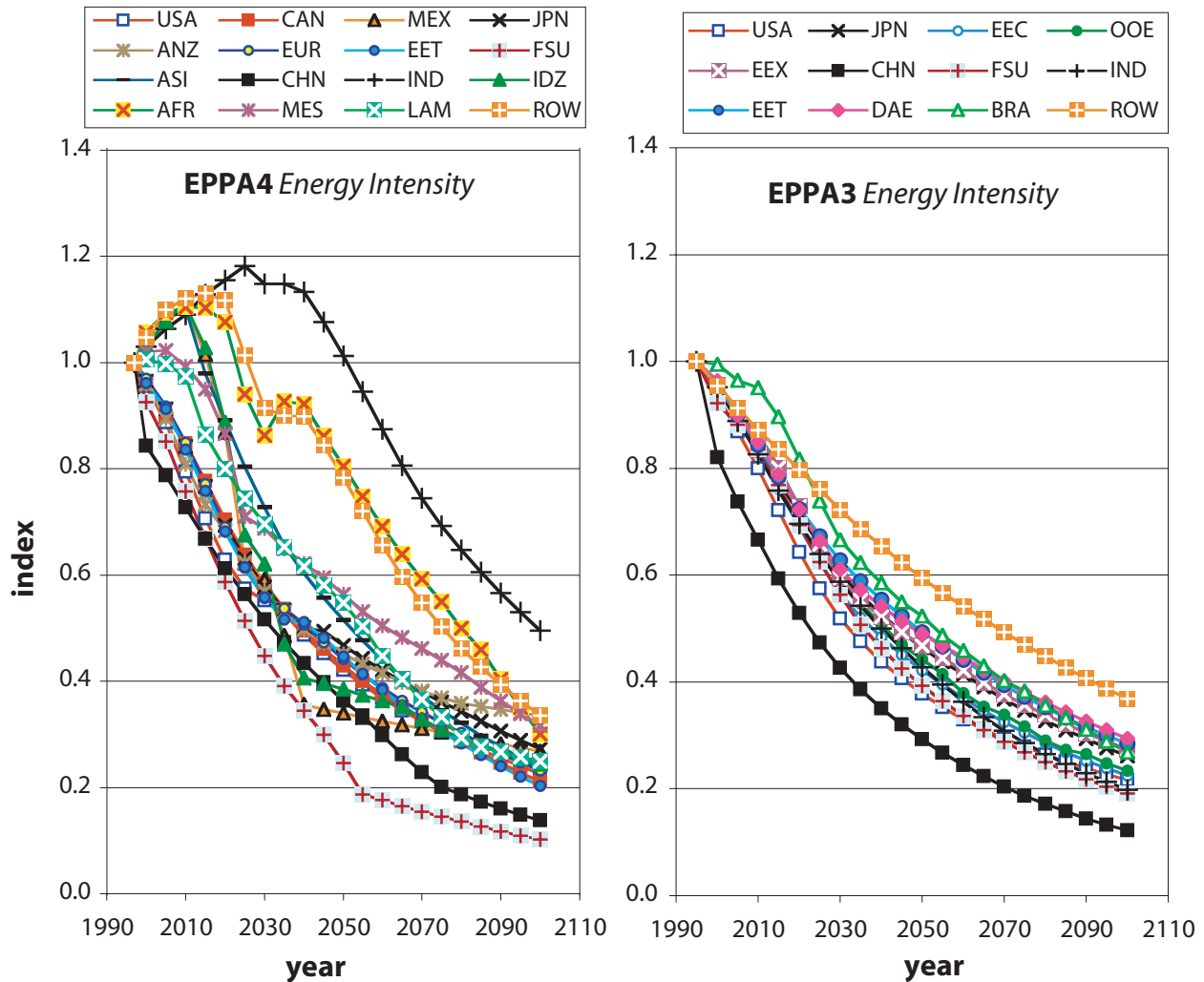
Figure 6. Energy intensity by region (see Table 1 for region abbreviations).

et al. (2001) this is not the case for many regions of developing countries where there has been little or no decline in energy intensity over the past 20 years. China is a major exception in that economic reforms appear to have been a catalyst for greatly improving efficiency. Both China and the FSU have inefficient energy-using capital stock compared with other regions, and so there is much room for improvement. The range of very different energy intensity changes in EPPA4 is more reflective of the variety of experiences in the recent historical record of different regions.

Another useful comparison between EPPA4 and EPPA3 is energy production by carbon-based fuel (**Figure 7**) and electric generation by technology and/or fuel (**Figure 8**). Two main differences in fuel production are: (1) total primary fuel production is considerably higher in EPPA4 than in EPPA3, up to 1250 EJ in EPPA4 from 880 EJ in EPPA3; and (2) liquid fuel from biomass supplies a substantial amount of fuel in EPPA4 (24% of liquid fuel production in 2100). Thus, addition of the liquid fuel from biomass technology option clearly has an important effect.
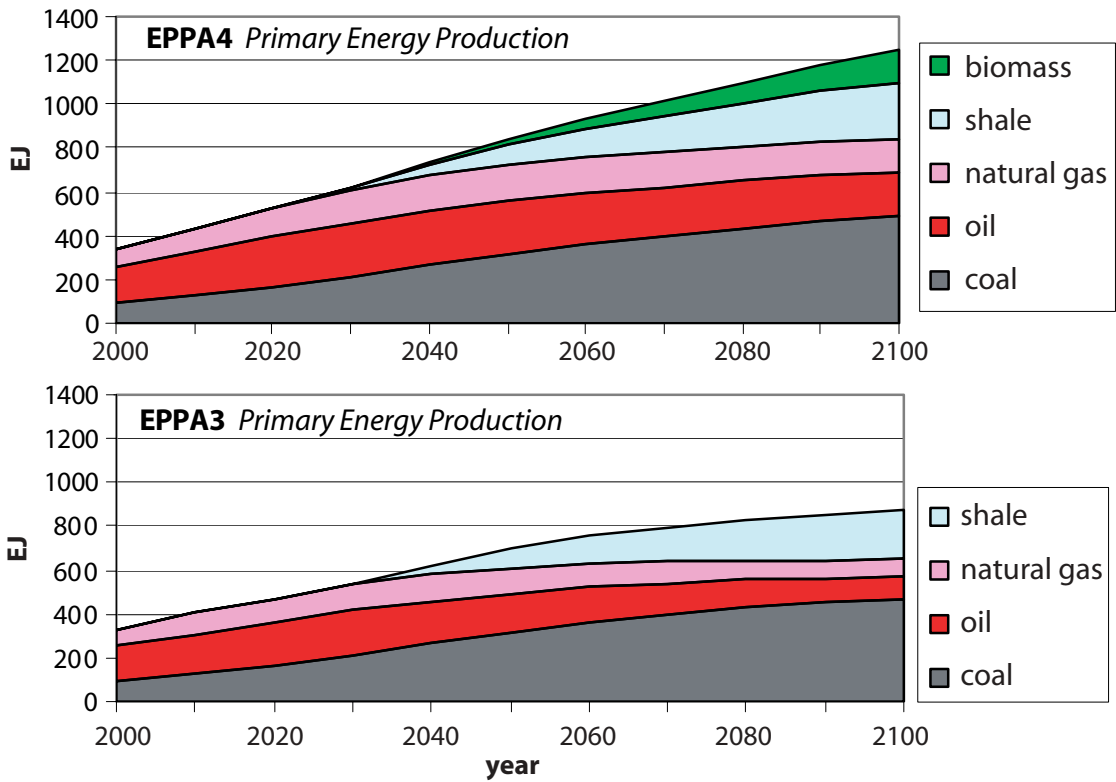
Figure 7. Primary energy production by type.
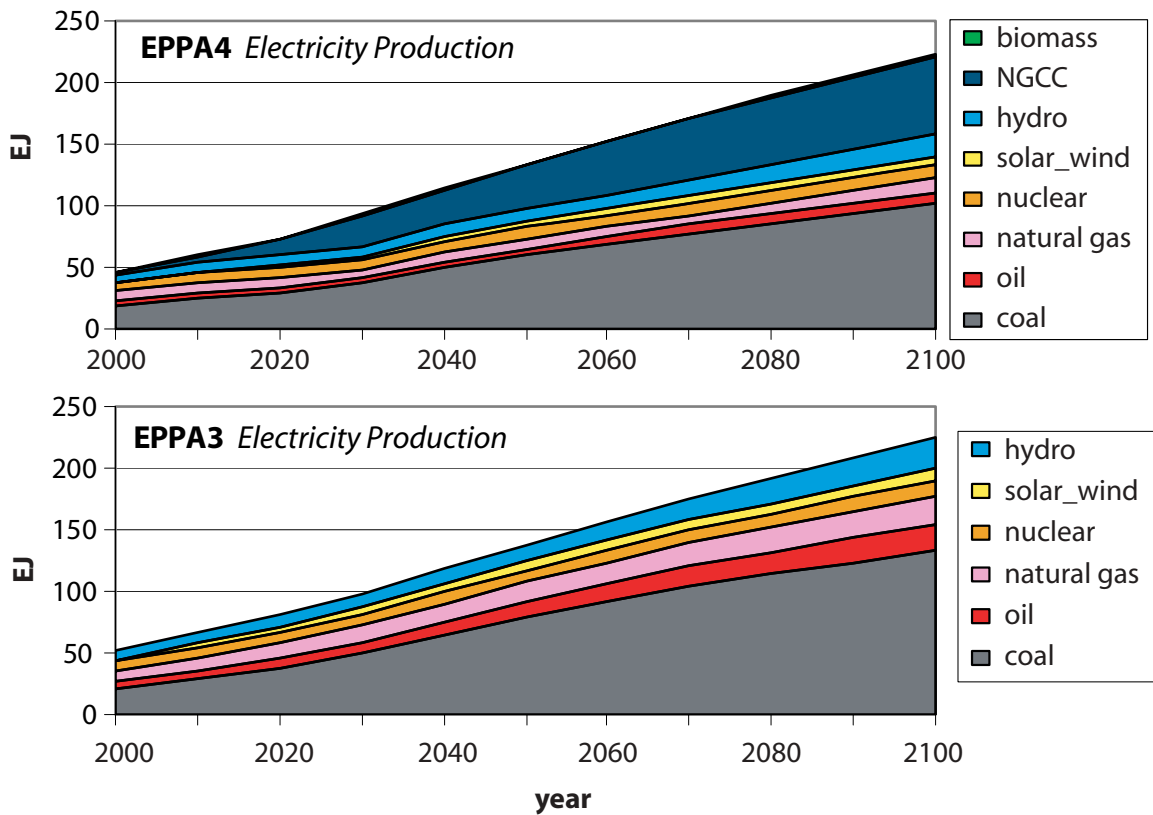
Figure 8. Electricity production by type.

Compared with EPPA3 there is more consumption in 2100 of each of the fossil fuels as well. Natural gas use in 2100 as projected by EPPA4 is twice that projected in EPPA3 and total liquid fuel use (shale, conventional oil including tar sands, and liquid fuel from biomass) is 80% greater in EPPA 4. Revisions to the resource model that made it easier to exploit the estimated available resources for gas and oil, and greater expansion of transportation demand for fuel by households due to explicit treatment of this sector, contributed to these changes.

Total electricity production (in exajoules, EJ, of electricity output) is little changed in EPPA4 compared with EPPA3 (Figure 8). In EPPA3, coal-based generation accounted for nearly 60% of electricity production in 2100; in EPPA4 its share is about 45%. A major reason for this change is that the newly added technology option, NGCC, accounts for 28% of generation. The significant contribution of NGCC is partly the result of revisions to the resource model that, particularly for regions with large gas resources, allows this gas to be produced at prices that make it competitive with other generation technologies. NGCC with capture and sequestration (NGCAP) and integrated coal gasification with capture and sequestration (IGCAP) do not enter in the reference scenario because the addition of the capture technology makes them uncompetitive with NGCC, or with direct use of coal for electricity generation, unless there is a positive price associated with emissions of CO_2.

The climatological effects of the changes in the greenhouse gas and other emissions projections resulting from revisions of the EPPA model were evaluated by running the IGSM1 for reference emission projections by EPPA3 and EPPA4. EPPA4 projections led to higher CO_2 and N_2O concentrations (**Figure 9**) but smaller CH_4 concentrations during most of the 21st century.
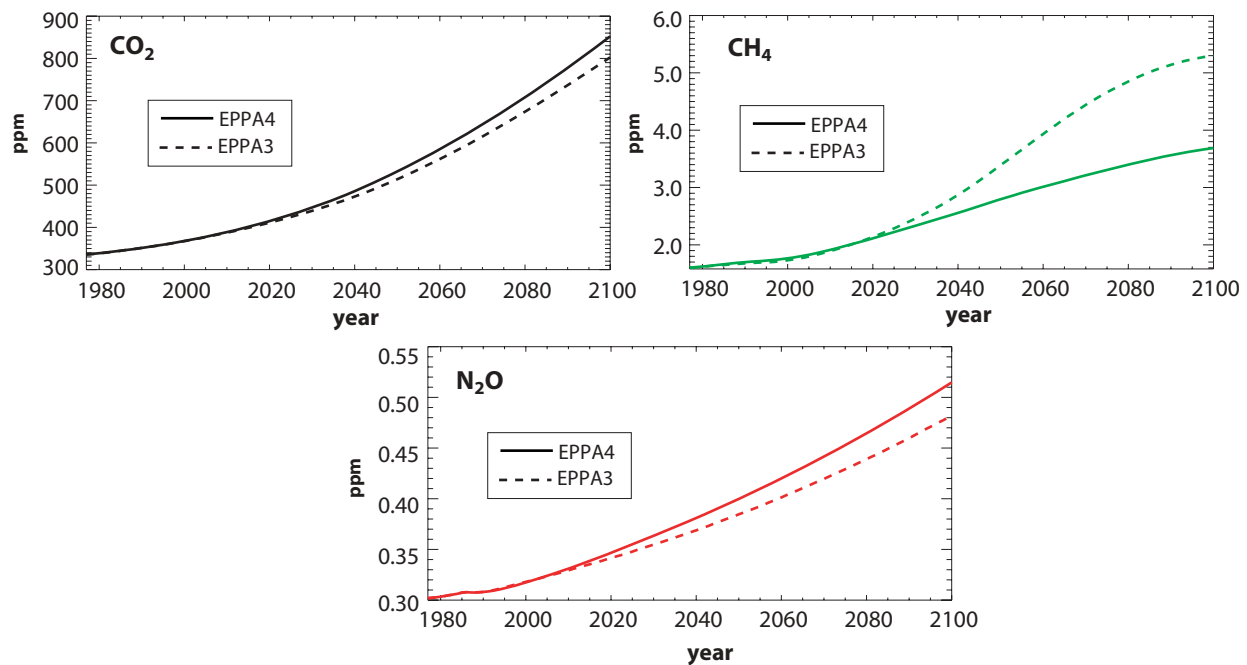
Figure 9. Atmospheric concentrations of CO_2 (black), CH_4 (green), and N_2O (red), in the simulations with emissions from EPPA3 (dashed lines) and EPPA4 (solid lines).

The resulting decrease in radiative forcing from methane was slightly larger than the increase in the forcing from higher levels of CO_2 (**Figure 10**). Changes in the forcings due to other gases and aerosols between EPPA4 and EPPA3 reference projections were smaller. The combined effects of all of the changes led, coincidentally, to virtually no change in total radiative forcing, and thus virtually no change in the projected global mean surface temperature.
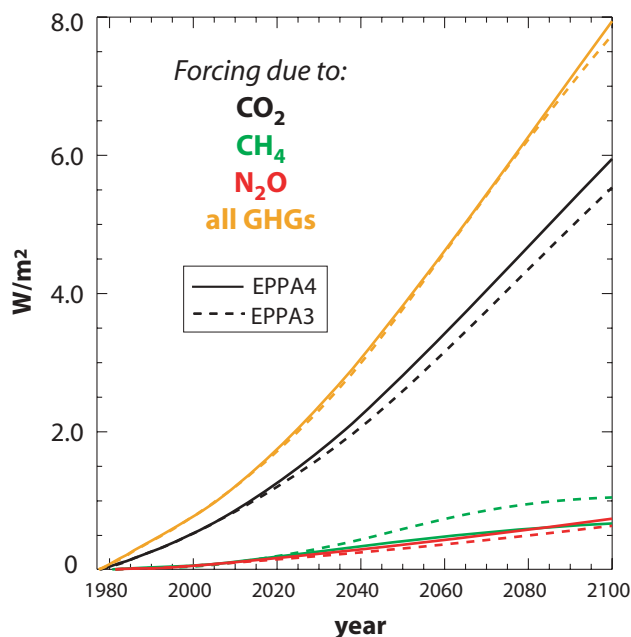
Figure 10. Radiative forcing due to CO_2 (black), CH_4 (green), N_2O (red) and all greenhouse gases (orange) in the simulations with emissions from EPPA3 (dashed lines) and EPPA4 (solid lines).

3.2 Comparison of Natural Science Components of the IGSM

Because of the large inertia of the ocean and carbon cycle models, a simulation of future climate should be begin from a pre-industrial equilibrium state of the climate system. As a result, the standard climate change simulation with the IGSM2 shown here was conducted in two stages: a simulation with historical forcings and a future climate projection. During the first stage, starting from 1860, the model was forced by the observed changes in greenhouse gas concentrations (Hansen *et al.*, 2002), tropospheric and stratospheric ozone (Wang & Jacob, 1998), the solar constant (Lean, 2000), sulfate aerosols (Smith *et al.*, 2004), and volcanic aerosols (Sato *et al.*, 1993). In simulations with the IGSM1 shown here, only changes in greenhouse gas concentrations, sulfate aerosol and ozone were taken into account.

For the historical forcing stage, carbon uptake by the ocean and terrestrial ecosystems are calculated but not fed back to the atmospheric model. Those uptakes were used to calculate an additional sink/source of carbon required to balance the carbon cycle. Based on data for anthropogenic carbon emissions and atmospheric CO_2 concentrations, the net land plus ocean carbon uptake should equal about 4.1 GtC/yr for the 1980s. The required additional sink/source

calculated to balance the carbon cycle was then kept constant during the subsequent forward simulations. Second-stage (forward) simulations with the full version IGSM2 were begun in 1991 (*c.f.* 1977 for IGSM1) using historical greenhouse gas emissions through 1996 and a reference emissions case as projected by EPPA4 for 1997 through 2100. For forward simulations all components of the IGSM2 were fully interactive; concentrations of all gases and aerosols were calculated by the atmospheric chemistry sub-model based on anthropogenic and natural emissions and terrestrial and oceanic carbon uptake. The IGSM2 includes the radiative effects of changes in concentrations of black carbon, while present-day black carbon values are used in radiative flux calculations in forward simulations with the IGSM1.

3.2.1 IGSM1 versus IGSM2.2

Surface air temperatures for 1861-2000 as simulated by IGSM1 and IGSM2.2 are compared with observations (Jones, 2003), as shown in **Figure 11**. Taking into account natural forcings, especially changes in stratospheric aerosol due to volcanic eruptions, has led to significantly better agreement with recent observations by IGSM2.2 compared to IGSM1. It should also be kept in mind that for this comparison IGSM1 was forced by observed changes in GHGs only until 1976 and then by EPPA4 emissions from 1977 to 1990, while IGSM2.2 used observations until 1990.

While post-1990 anthropogenic emissions are identical in both simulations in Figure 11, there are some differences in both oceanic and terrestrial carbon uptakes (**Figure 12**) as well as in the
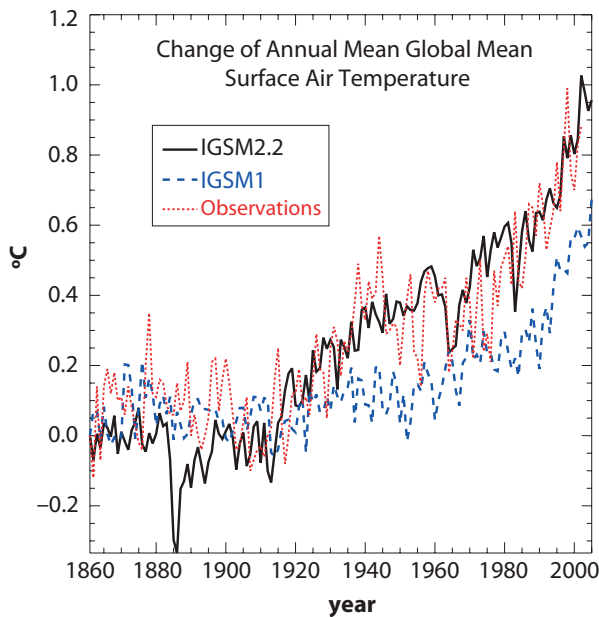
Figure 11. Changes in global mean annual mean surface air temperature in simulations with IGSM1 (dashed blue line) and IGSM2.2 (black line). Observations (dotted red line) are from Jones (2003).
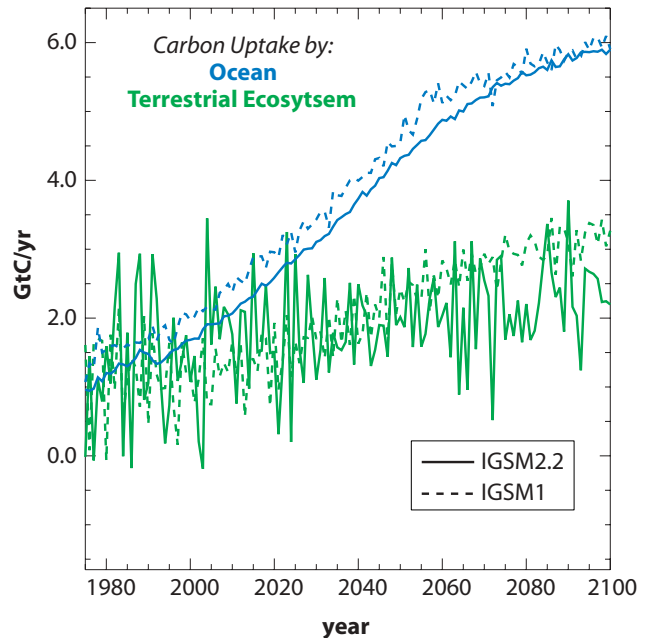
Figure 12. Carbon uptake by ocean (blue) and terrestrial ecosystem (green) in the simulations with the IGSM2.2 (solid lines) and IGSM1 (dashed lines).

natural emissions of CH_4 and N_2O (**Figure 13**). As a result, GHG concentrations in the two simulations are also different (**Figure 14**). Those differences are, however, too small to significantly affect radiative forcing (**Figure 15**). Forcing due to sulfate aerosols, while similar in the spin-up stage of the two simulations, becomes noticeably different after 1997 (**Figure 16**). This difference is caused by the difference in estimates of SO_2 emissions over the period 1977-1997 in the Version 1 and 2 IGSM simulations. IGSM1 simulations kept SO_2 emissions constant at the EPPA-predicted 1997 level for the entire period from 1977 to 1996. A more realistic historical pattern of SO_2 emissions was used in the IGSM2 simulation.

The coefficient of total sulfate aerosol radiative forcing efficiency used during the second stage of the simulation (see Webster *et al*., 2003) was chosen so as to produce aerosol forcing of –0.6 W/m^2 for the 1980s and was different in the IGSM1 and IGSM2. This led to aerosol forcing in the last part of the simulation with the IGSM1 being about –0.1 W/m^2 smaller than for the
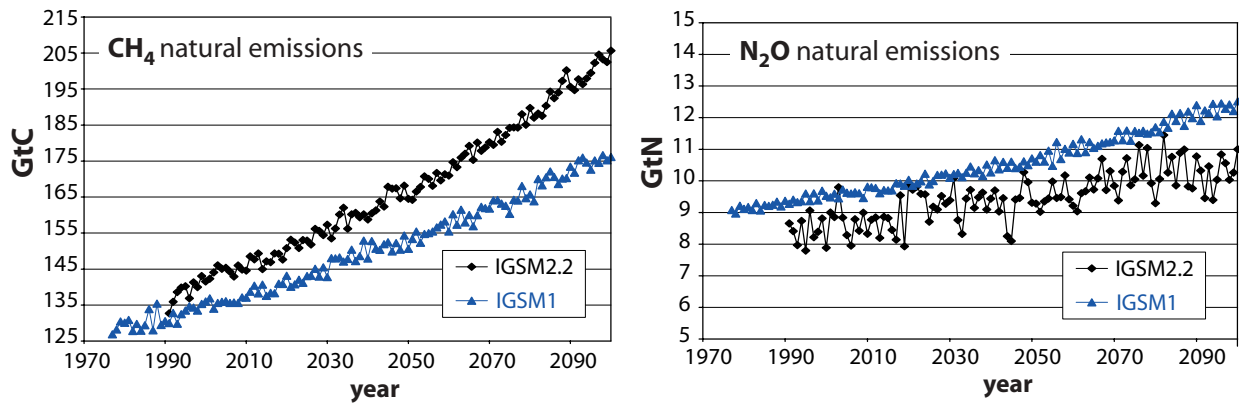
Figure 13. Natural emissions of CH_4 and N_2O in the simulations with the IGSM1 and IGSM2.2.
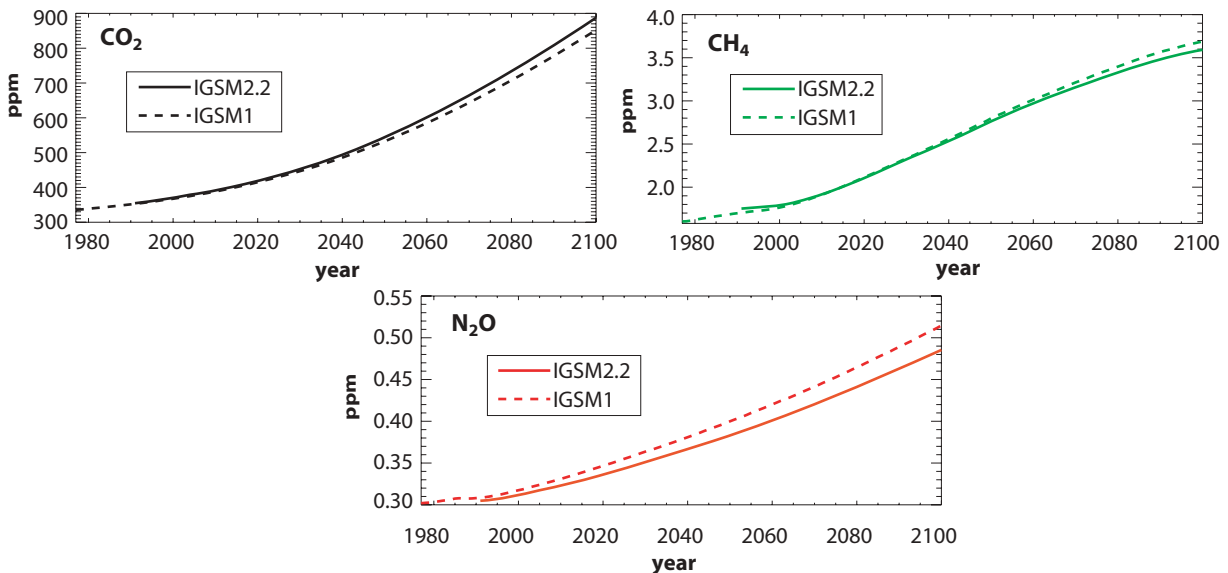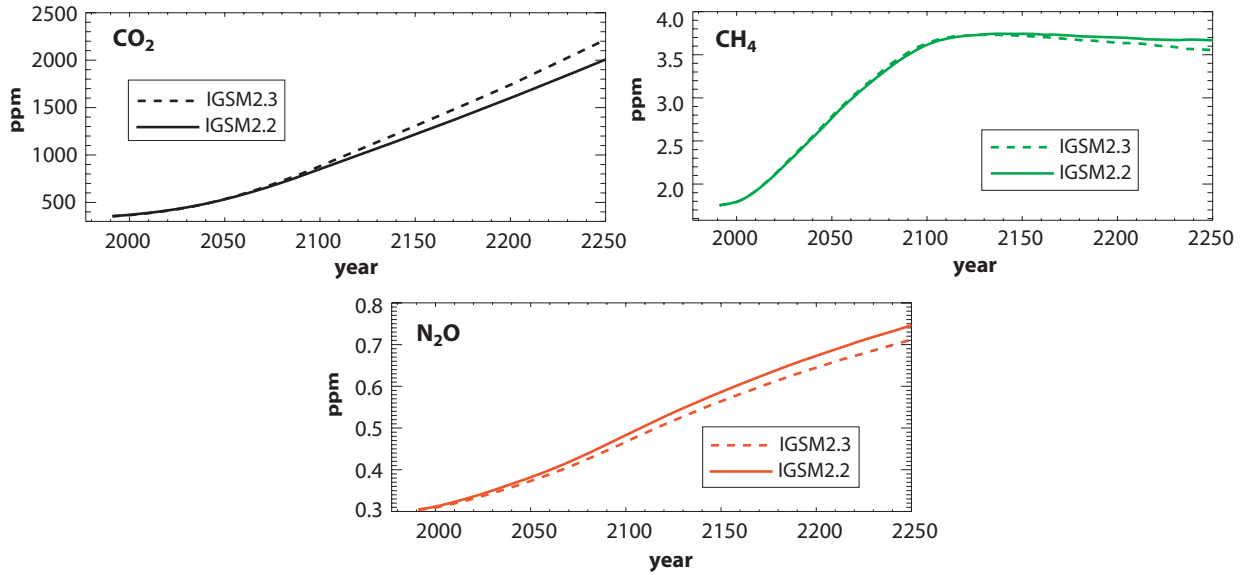

Figure 14. Atmospheric concentrations of CO_2 (black), CH_4 (green) and N_2O (red) in the simulations with the IGSM2.2 (solid lines) and IGSM1 (dashed lines).
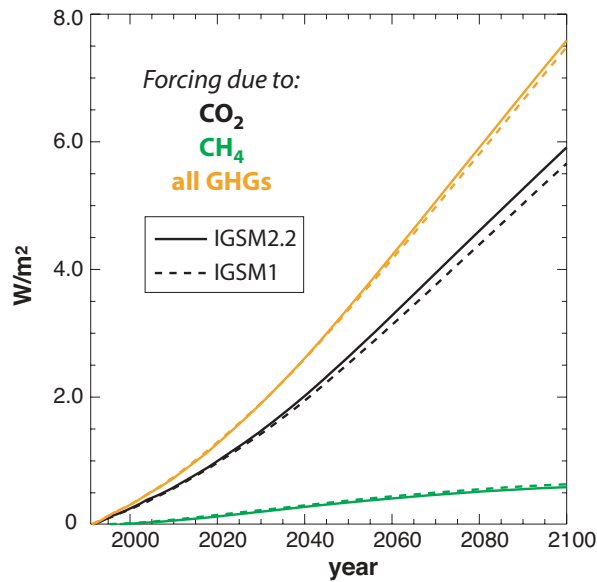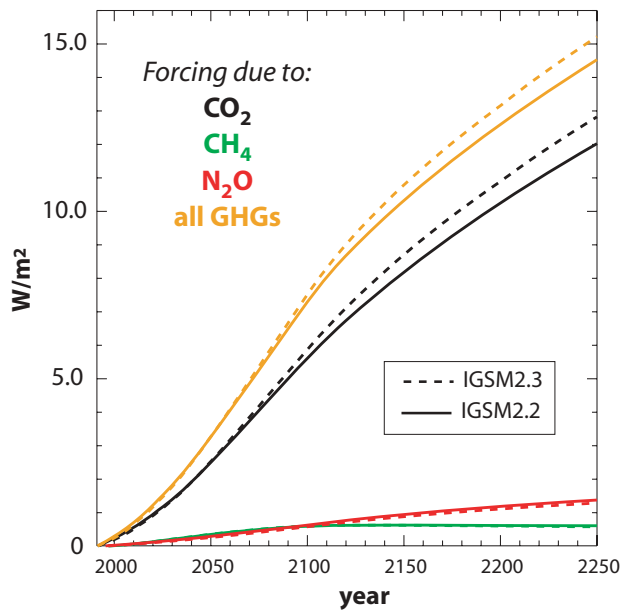
Figure 15. Radiative forcing due to CO_2 (black), CH_4 (green), and all greenhouse gases (orange) in the simulations with the IGSM2.2 (solid lines) and IGSM1 (dashed).
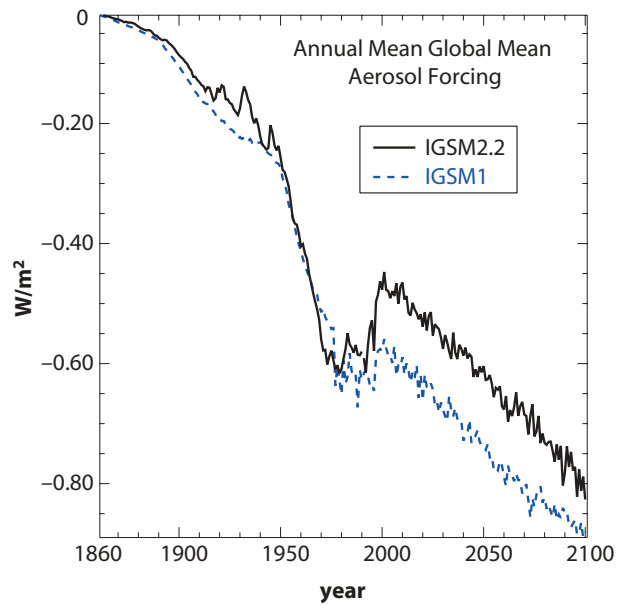
Figure 16. Radiative forcing due to sulfate aerosol in the simulations with the IGSM2.2 (solid black line) and IGSM1 (dashed blue line).

IGSM2. This difference is small compared to the greenhouse gas forcings. At the same time, taking into account changes in the concentration of black carbon aerosol produces an additional surface warming of about 0.5 °C over the 110 year period from 1990 to 2100 (**Figure 17**).

There are substantial differences in sea level rise due to thermal expansion and changes in sea-ice cover between the IGSM1 and IGSM2.2 simulations. Differences in sea level rise
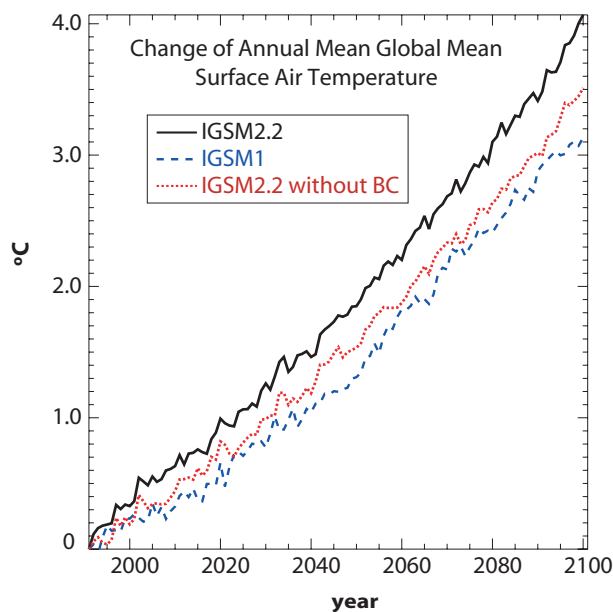
Figure 17. Changes in global mean annual mean surface air temperature in simulations with IGSM1(dashed blue line), IGSM2.2 (solid black line), and IGSM2.2 without including the radiative effect of black carbon (dotted red line).

(**Figure 18**), at least in part, are associated with the fact that in the simulation with the IGSM2.2 surface air temperature rises by about 1 ºC from 1900 to 2000 compared to only 0.5 °C in the simulation with the IGSM1 (Figure 11). This results in a longer and deeper penetration of the warming into the ocean during the entire IGSM2.2 simulation. Differences in sea-ice melting (**Figure 19**) on the other hand are associated with the differences in the model structures. The use of a zonally averaged mixed-layer ocean model results in unrealistically abrupt changes in sea ice in the simulation with the IGSM1. Sea-ice behavior is simulated much better by the IGSM2.2, which as noted in Section 2.4.1 incorporates a 2D (latitude by longitude) version of the ocean mixed-layer.

Figure 20 shows changes in the zonal mean distributions of some key climate variables between the decades of 1981-1990 and 2091-2100. The IGSM1 produces less warming in the equatorial region and larger polar amplification of climate changes than the IGSM2.2. Differences in the zonal mean distribution of changes in surface air temperature are consistent with the larger decrease of surface albedo in the simulation with the IGSM1. The latter albedo difference is, to large extent, associated with the differences in sea ice and snow cover between the IGSM versions. Differences in the snow-free land albedo are minor in spite of the use of different land models in the two versions of the IGSM. Changes in precipitation are rather similar in both simulations. Based on the results of some preliminary simulations, the different pattern near the equator is due to the difference in horizontal resolution. Differences in evaporation at low latitudes occur mainly over the ocean and are related to the larger surface
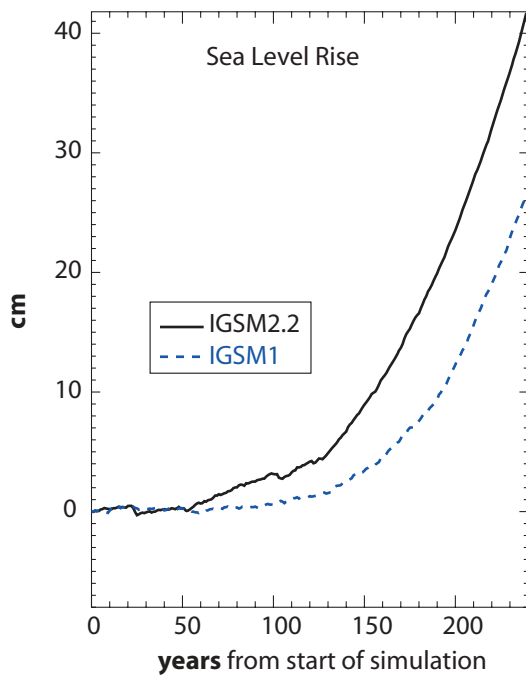
Figure 18. Sea level rise due to thermal expansion in simulations with IGSM1 (dashed blue) and IGSM2.2 (solid line).
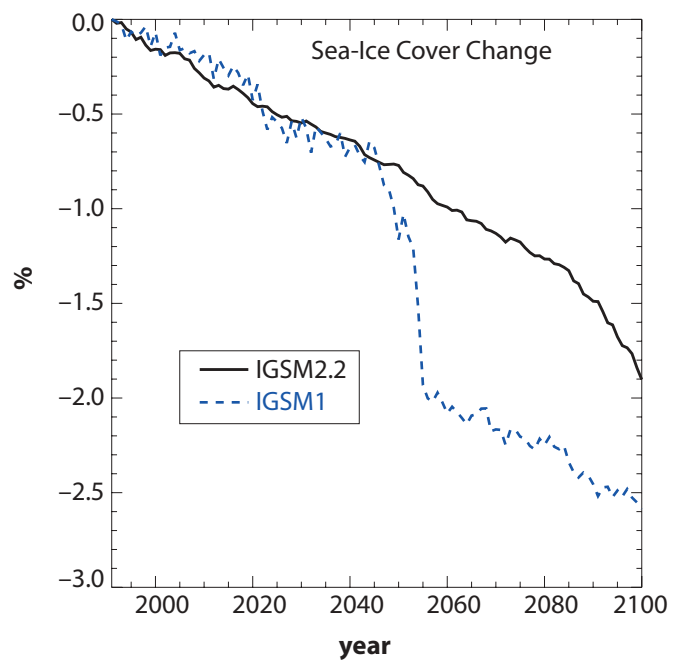
Figure 19. Sea-ice cover change (from 1990) in simulations with IGSM1 (dashed blue line) and IGSM2.2 (solid black line).

27
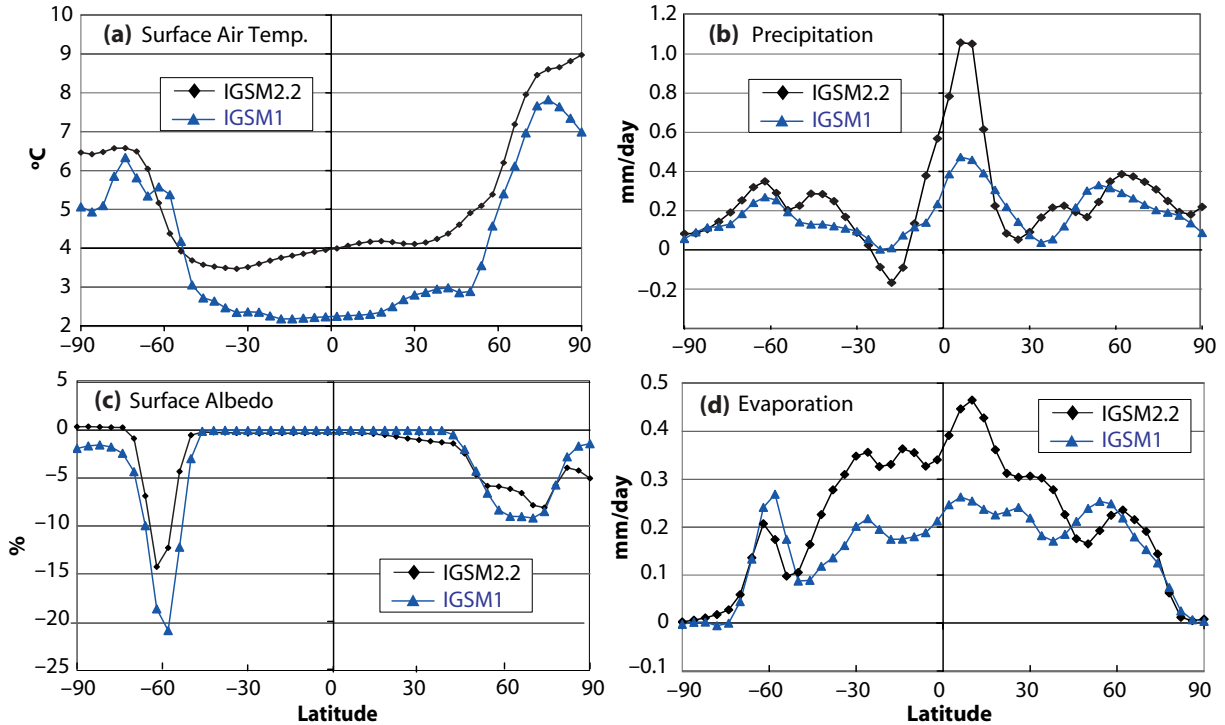
Figure 20. Changes in zonally averaged (a) surface air temperature, (b) precipitation, (c) surface albedo, and (d) evaporation. Difference between decadal means 2091-2100 and 1981-1990.

warming in IGSM2.2. The increases in evaporation over land are quite similar in the two IGSM versions, except in the northern high latitudes, even though the representation of land processes was substantially revised.

3.2.2 IGSM2.2 versus IGSM2.3

As shown by Sokolov *et al.* (2003), the versions of the MIT 2D climate model (IGSM1, and also IGSM2.2) with a mixed-layer/diffusive ocean model can (with an appropriate choice of the vertical diffusion coefficient and climate sensitivity) simulate well the behavior of any coupled AOGCM, in terms of surface warming and sea level rise, on time scales of about 100-150 years. From a simulation with 1% per year increase in the atmospheric CO_2 concentration the effective diffusion coefficient and climate sensitivity for the IGSM2.3 were found to be 4 cm^2s^{-1} and 2 ºC respectively. These values were then used in the simulation with the IGSM2.2 discussed in this section so that the overall behavior of the IGSM2.2 model should replicate that of the IGSM2.3 model. As can be seen from **Figure 21**, the simpler IGSM2.2 indeed matches closely the change in surface air temperature simulated by the IGSM2.3 for a more than 300-year forward simulation. For these simulations, both models were run from 1861 to 2100 as described previously; the integrations were then continued for another 150 years with anthropogenic emissions fixed at their values in 2100.

While there is good agreement in projected surface warming, IGSM2.2 begins to overestimate sea level rise due to thermal expansion of the ocean after 200 years of integration (**Figure 22**).
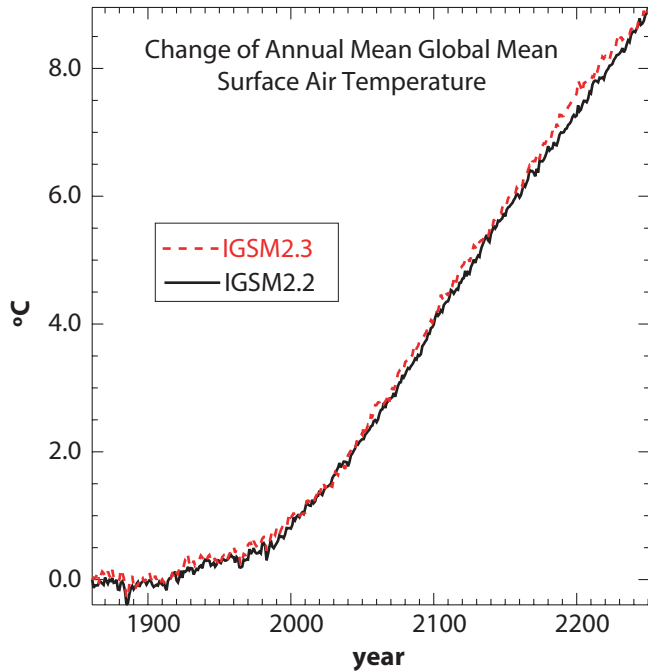
Figure 21. Changes in global mean annual mean surface air temperature in simulations with IGSM2.2 (solid line), IGSM2.3 (dashed red).
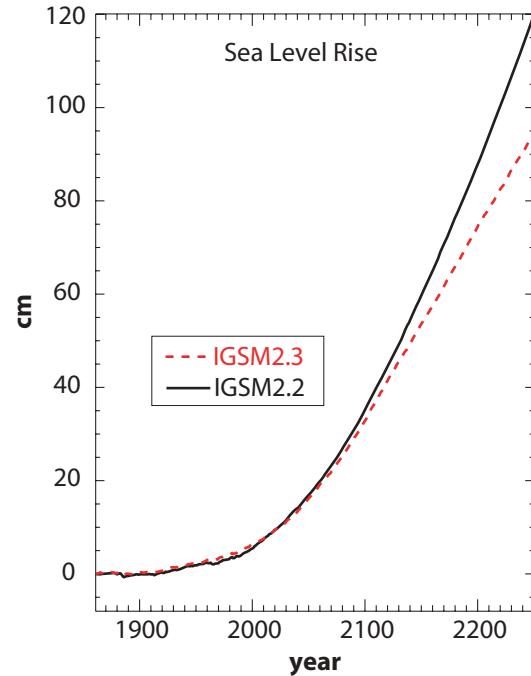
Figure 22. Changes in sea level rise due to thermal expansion in simulations with IGSM2.2 (solid), IGSM2.3 (dashed red).

Hence, while the mixed-layer/diffusive ocean model can simulate well the overall heat uptake by the deep ocean, apparently it cannot describe changes in the structure of the deep ocean temperature on long time scales. However, as shown by Sokolov & Stone (1998), the mixed-layer model does simulate such changes on shorter time-scales quite well.

While ocean carbon models in both versions of the model include parameterization of the solubility pump, the IGSM2.2 has no representation of the ocean biology nor is it capable of simulating the feedbacks between changes in ocean circulation and carbon uptake by the ocean. This leads to significant differences in the carbon cycle simulated by the IGSM2.2 and IGSM2.3 up to 2100. In the simulation with the IGSM2.2, carbon uptake by the ocean increases almost linearly up to year 2100 and then decreases after that (**Figure 23**). In contrast, in the IGSM2.3 simulation it reaches a maximum of about 5 GtC/yr around 2050 and then starts to decrease despite continuing increases in CO_2 emissions until 2100. Because CO_2 is less soluble in warmer water, the ocean solubility pump becomes less efficient with the increase in the sea surface temperature, limiting carbon uptake by the ocean. Several authors have cited this as the major feedback mechanism in the ocean carbon cycle (Matear *et al.*, 1999, Chuck *et al.*, 2005). Changes to the ocean circulation (Sarmiento *et al.*, 1998; Chuck *et al.*, 2005; Matear & Hirst, 1999) and potentially decreased biological productivity (Chuck *et al.*, 2005) can also lead to the reduced ability of the ocean to take up carbon. As discussed by Dutkiewicz *et al.* (2005), in the pre-industrial steady-state some parts of the ocean out-gassed CO_2 and some areas took up
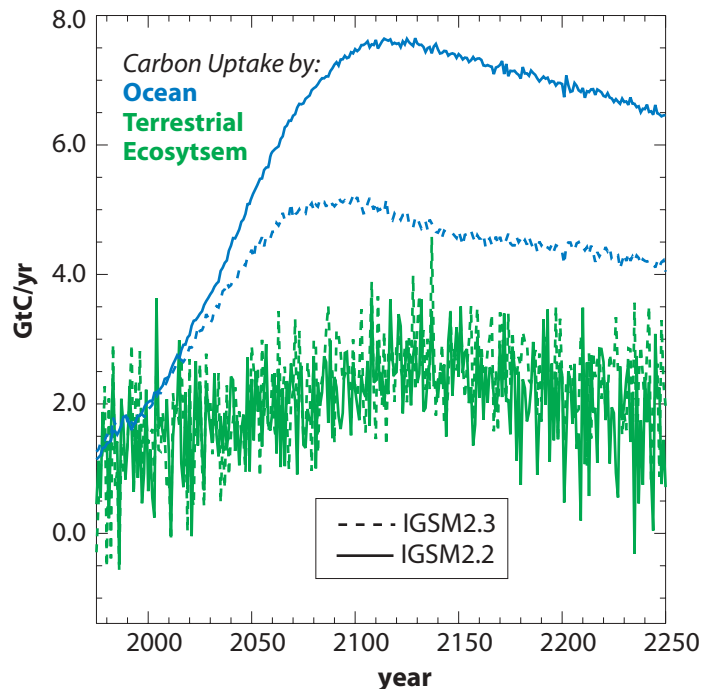
Figure 23. Changes in oceanic (blue) and terrestrial (green) carbon uptake in the simulations with IGSM2.2 (solid lines), IGSM2.3 (dashed lines).

carbon. By 2050, the areas of out-gassing have almost all switched to regions of uptake, and the rate at which the global ocean can take up CO_2 thus levels off.

Carbon uptake by the terrestrial ecosystem is practically identical in both simulations with a slow increase in uptake until around 2125 and then a decrease after that, similar to the ocean uptake behavior. The differences in the ocean sinks result in CO_2 concentrations in the year 2250 (**Figure 24**) that are about 200 ppm higher in the IGSM2.3 simulation than in IGSM2.2. Due to logarithmic dependency of radiative forcing on CO_2 concentration, the differences in forcing (**Figure 25**) are too small to have a noticeable effect on the climate projections of the two model versions.

After 2100, when anthropogenic emissions are fixed, the rate of increase in the radiative forcing naturally starts to decrease. This change in the forcing is almost immediately reflected in the behavior of the meridional overturning circulation of the ocean (**Figure 26**). While decreasing rather quickly during the 21st century, the overturning begins to recover once emissions cease increasing. However with emissions constant, atmospheric CO_2 concentrations continue to increase and eventually force the meridional overturning to slow down again. Similar behavior of the overturning circulation was observed in a simulation carried out with the IGSM2.3 driven by the SRES A2 emission scenario for the IPCC Assessment Report 4 Working Group 1 model intercomparison.

Figure 24. Atmospheric concentrations of CO_2 (black), CH_4 (green) and N_2O (red) in the simulations with the IGSM2.2 (solid lines) and IGSM2.3 (dashed lines).

Figure 25. Radiative forcing due to CO_2 (black), CH_4 (green), N_2O (red) and all greenhouse gases (orange) in simulations with the IGSM2.2 (solid lines) and IGSM2.3 (dashed).
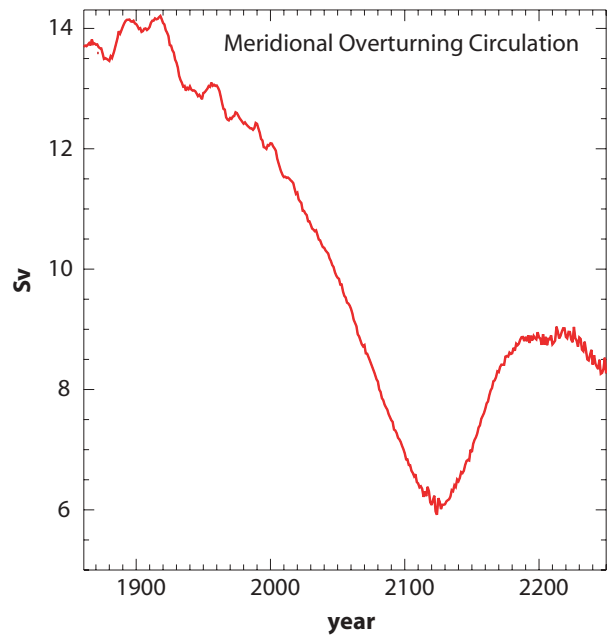
Figure 26. Change in the meridional overturning circulation in the North Atlantic in the simulation with the IGSM2.3.

Finally, we note that zonally-averaged distributions of changes in different climate variables as simulated by IGSM2.2 and IGSM2.3 (**Figure 27**) are overall very close except in the polar regions. The differences in sea-ice cover are, to large part, related to differences in how the flux adjustment is calculated in the IGSM2.2 and IGSM2.3. As stated earlier, in the spin-up simulation with the IGSM2.2, both sea surface temperature and sea ice are relaxed toward the
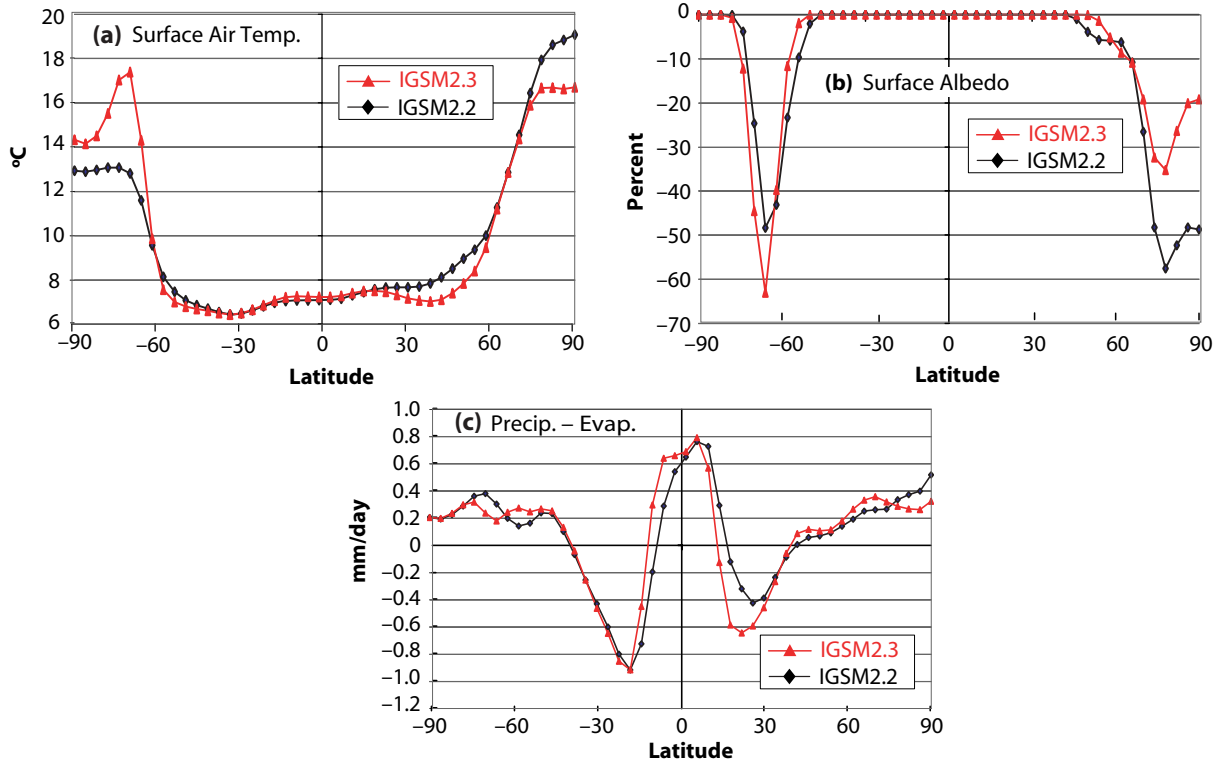
Figure 27. Changes in zonally averaged (a) surface air temperature, (b) sea-ice cover, and (c) precipitation minus evaporation in simulations with IGSM2.2 and IGSM2.3. Difference between decadal means 2241-2250 and 1981-1990.

observations, while in the IGSM2.3 spin-up relaxation is applied to temperature only. As a result, sea-ice cover in the equilibrium pre-industrial climate simulations with the IGSM2.2 and IGSM2.3, as well as sea-ice changes in the simulations discussed above, are somewhat different.

4. CLOSING REMARKS

A large number of improvements have been made to the revisions and extensions leading to the IGSM2. To summarize:

Emissions Projections. The achievements in the EPPA component are discussed in Section 2.1 and detailed further by Paltsev *et al.* (2005). They include a more complete treatment of technology and material flows, greater geographic disaggregation and sectoral detail, expanded specification of energy technologies, updated economic and emissions data, expanded capabilities for policy analysis, and updated linkages to the earth system sub-models.

Climate system response. So far as climate system response is concerned, IGSM2.2/2.3 provides a significantly better simulation of climate change since pre-industrial time than IGSM1. Shortcomings of IGSM1, such as unrealistically abrupt changes in sea-ice cover or overheating of land surface in the mid-latitudes of the Northern Hemisphere during local summer, were eliminated by developing new ocean and land surface models as well as by an increase in horizontal resolution of the atmospheric model. The development of new versions of

the terrestrial ecosystem and natural emissions models also eliminated recognized inconsistencies in descriptions of the hydrological cycle and surface energy budget among the land components of the IGSM.

Incorporation of a 3D ocean model into the IGSM framework has led to significant improvements in the simulated deep ocean circulation and carbon cycle, and enables us to carry out more realistic longer-term climate change simulations (greater than 150 years), which could involve changes in the thermohaline circulation. At the same time, comparisons of IGSM2.3 and the computationally much less demanding IGSM2.2 show that the latter model simulates reasonably well many aspects of possible climate change through the end of the 21st century. It thus allows us to credibly perform uncertainty studies with the IGSM2.2, which require carrying out very large numbers of simulations.

Feedbacks and interactions. In addition to the system components for human emissions and climate system response, substantial advances have been made in the ability to represent the many and complex feedbacks among these processes. These advances involve four general areas: (1) feedback effects of ozone damage and its effects on carbon storage in terms of increased cost of meeting a concentration target (Felzer *et al*., 2004, 2005); (2) evaluation of the human health impacts of air pollution and interaction with climate policy (Yang *et al.*, 2004, 2005; Matus *et al.,* 2005; Matus, 2005); (3) evaluation of the multiple environmental changes (CO_2, climate, tropospheric ozone) on crop yields and feedbacks on the global economy and agricultural trade (Reilly *et al.*, 2004; Wang, 2005); and (4) elucidating the effects of air pollution policy on climate (Prinn *et al*., 2005). These advances particularly emphasize the linkage of changes in climate and atmospheric composition on the economy, a capability that did not exist in IGSM Version 1.

A major direction for further development of the IGSM is a tighter integration of the EPPA component with the earth system components of the model. This builds further on the development of key material flows and balances added to EPPA. One key linkage is the demographic model that simulates the spatial distribution of population to identify the changing geographic pattern of emissions, as well as to track exposure of the population to pollution. The approach that has been developed and evaluated makes the geographic population distribution a function of economic variables projected by EPPA (Asadoorian, 2005). This component is in the process of being introduced into the IGSM code, for further evaluation and testing. This will facilitate linkage with the urban air pollution component and further study of the air pollution health effects and feedbacks on the economy. The other key linkage that is being developed is between the EPPA and TEM components. The objective of this work is to dynamically link these components to simulate interactive effects of environmental change on vegetation (including crops, forest, pasture/grazing land, and bioenergy crops) the resulting effects on agriculture and energy production and trade, and the feedback on land use and emissions of greenhouse gases from land-use change.

Acknowledgements

5. REFERENCES

Andronova, N.G., and M.E. Schlesinger, 2001. Objective estimation of the probability density function for climate sensitivity. *J. Geophysical Research*, **106**(D19): 22,605-22,612.

Asadoorian, M., 2005. *Simulating the Spatial Distribution of Population and Emissions to 2100.* Report 123, MIT Joint Program on the Science and Policy of Global Change, Cambridge, MA (available at http://mit.edu/globalchange/www/MITJPSPGC_Rpt123.pdf).

Asadoorian, M., J. Tay, A. Valpergue de Masin, K. See, R. Sandoval, S. Paltsev and J. Reilly, 2005. *Emissions Inventories and Time Trends for Greenhouse Gases and other Pollutants.* MIT Joint Program on the Science and Policy of Global Change Report, forthcoming.

Babiker, M.H., J.M. Reilly, M. Mayer, R.S. Eckaus, I. Sue Wing and R.C. Hyman, 2001. *The MIT Emissions Prediction and Policy Analysis (EPPA) Model: Revisions, Sensitivities, and Comparisons of Results.* Report 71, MIT Joint Program on the Science and Policy of Global Change, Cambridge, MA (http://mit.edu/globalchange/www/MITJPSPGC_Rpt71.pdf).

Bitz, C.M., and W.H. Lipscome, 1999. An energy conserving thermodynamic model of sea ice. *J. Geophysical Research*, **104**: 15,669-15,677.

Bonan, G.B., K.W. Oleson, M. Vertenstein, S. Lewis, X. Zeng, Y. Dai, R.E. Dickinson and Z.-L. Yang, 2002. The land surface climatology of the Community Land Model coupled to the NCAR Community Climate Model. *J. Climate*, **15**: 3123-3149.

Byun, D.W., S. Zhang, B. Lefer, B. Rappenglueck, J. He, H.-J. In, S. Kim, P. Percell and C.-K. Song, 2005. *Comprehensive Air Quality Model with Extensions*. Institute for Multidimensional Air Quality Studies, University of Houston (http://www.imaqs.uh.edu/).

Calbó, J., W. Pan, M. Webster, R.G. Prinn and G.J. McRae, 1998. Parameterization of urban sub-grid scale processes in global atmospheric chemistry models. *J. Geophysical Research*, **103**: 3437-3451.

Chen, Y., and R. Prinn, 2005. Atmospheric modeling of high frequency methane observations: Importance of interannually varying transport. *J. Geophysical Research,* **110**: D10303.

Chen, Y., 2003. *Estimation of Methane and Carbon Dioxide Surface Fluxes using a 3-D Global Atmospheric Chemical Transport Model*. Ph.D. Thesis, MIT, Report No. 73, MIT Center for Global Change Science (http://mit.edu/cgcs/www/MIT_CGCS_Rpt73.html), 180p.

Chuck, A., T. Tyrrell, I.J. Totterdell and P.M. Holligan, 2005. The oceanic response to carbon emissions over the next century: Investigation using three ocean carbon cycle models. *Tellus B*, **57**: 70-86.

CIESIN (Center for International Earth Science Information Network), Columbia University; International Food Policy Research Institute (IFPRI); and World Resources Institute (WRI), 2000. *Gridded Population of the World (GPW), Version 2*. Palisades, NY: CIESIN, Columbia University (http://sedac.ciesin.columbia.edu/plue/gpw).

Claussen, M., L.A. Mysak, A.J. Weaver, M. Crucifix, T. Fichefet, M.-F. Loutre, S.L. Weber, J. Alcamo, V.A. Alexeev, A. Berger, R. Calov, A. Ganopolski, H. Goosse, G. Lohman, F. Lunkeit, I.I. Mokhov, V. Petoukhov, P. Stone and Z. Wang, 2002. Earth system models of intermediate complexity: Closing the gap in the spectrum of climate system models. *Climate Dynamics*, **15**: 579-586.

Colman, R., 2003. A comparison of climate feedbacks in general circulation models. *Climate Dynamics*, **20**: 865-873.

Dai, A., W.M. Washington, G.A. Meehl, T.W. Bettge and W.G. Strand, 2004: The ACPI climate change simulations. *Climatic Change*, **62**: 29-43.

Dai, Y., X. Zeng, R.E. Dickinson, I. Baker, G. Bonan, M. Bosilovich, S. Denning, P. Dirmeyer, P. Houser, G. Niu, K. Oleson, A. Schlosser and Z.-L. Yang, 2003. The Common Land Model (CLM). *Bulletin of the American Meteorological Society*, **84**: 1013-1023.

Dalan, F., P.H. Stone, I. Kamenkovich and Scott, 2005a. Sensitivity of the ocean's climate to diapycnal diffusivity in EMIC. Part I: Equilibrium state. *J. Climate*, **18**: 2460-2481 (see also http://mit.edu/globalchange/www/MITJPSPGC_Rpt109.pdf).

Dalan, F., P.H. Stone and A.P. Sokolov, 2005b. Sensitivity of the ocean's climate to diapycnal diffusivity in EMIC. Part II: Global warming scenario. *J. Climate*, **18**: 2482-2496.

DOE, 1994. *Handbook of methods for the analysis of various parameters of the carbon dioxide system in sea water (Version 2).* A.G. Dickson and C. Goyet (eds.), ORNL/CDIAC-74.

Dimaranan, B., and R. McDougall, 2002. *Global Trade, Assistance, and Production: The GTAP 5 Data Base.* Center for Global Trade Analysis, Purdue University, West Lafayette, Indiana.

Duffy, P.B., B. Govindasamy, J.P. Iorio, J. Milovich, K.B. Sperber, K.E. Taylor, M.F. Wehner, and S.L. Thompson, 2003. High resolution simulations of global climate. Part 1: Present climate. *Climate Dynamics*, **21**: 371-390.

Dutkiewicz. S., A. Sokolov, J. Scott and P. Stone, 2005. *A Three-Dimensional Ocean-Seaice-Carbon Cycle Model and its Coupling to a Two-Dimensional Atmospheric Model: Uses in Climate Change Studies.* Report 122, MIT Joint Program on the Science and Policy of Global Change (http://mit.edu/globalchange/www/MITJPSPGC_Rpt122.pdf).

Felzer, B., J. Reilly, J. Melillo, D. Kicklighter, M. Sarofim, C. Wang, R. Prinn and Q. Zhuang, 2005. Future effects of ozone on carbon sequestration and climate change policy using a global biogeochemical model. *Climatic Change*, in press (see also http://mit.edu/globalchange/www/MITJPSPGC_Rpt103.pdf).

Felzer, B., D.W. Kicklighter, J.M. Melillo, C. Wang, Q. Zhuang and R. Prinn, 2004. Effects of ozone on net primary production and carbon sequestration in the conterminous United States using a biogeochemistry model. *Tellus B*, **56**: 230-248.

Forest, C. E., P.H. Stone, A.P. Sokolov, M.R. Allen, and M. Webster, 2002: Quantifying uncertainties in climate system properties with the use of recent climate observations. *Science*, **295**: 113-117.

Forest, C.E., M.R. Allen, A.P. Sokolov and P.H. Stone, 2001. Constraining climate model properties using optimal fingerprint detection methods. *Climate Dynamics*, **18**: 277-295.

Forest, C.E., M.R. Allen, P.H. Stone and A.P. Sokolov, 2000. Constraining uncertainties in climate models using climate change detection techniques. *Geophysical Research Letters*, **27**: 569-572.

GEIA (Global Emissions Inventory Activity), 2005. Review of CFC-11 & CFC-12: Metadata on Distributed Emissions (http://www.geiacenter.org/reviews/cfc11.html, and http://www.geiacenter.org/reviews/cfc12.html).

Gent, P., and J. McWilliams, 1990. Isopycnal mixing in ocean circulation models. *J. Physical Oceanography*, **20**: 150-155.

Govindasamy, B., P.B. Duffy and J. Coquard, 2003. High-resolution simulations of global climate. Part 2: Effects of increased greenhouse gases. *Climate Dynamics,* **21**: 391-404.

Gregory, J.M., K.W. Dixon, R.J. Stouffer, A.J. Weaver, E. Driesschaert, E. Eby, T. Fichefet, H. Hasumi, A. Hu, J. Jungclause, I.V. Kamenkovich, A. Levermann, M. Montoya, S. Murakami, S. Nawrath, A. Oka, A. Sokolov and R.B. Trorpe, 2005. A model intercomparison of changes in the Atlantic thermohaline circulation in response to increasing atmospheric CO_2 concentration. *Geophysical Research Letters*, **32**(12): L12703.

Gregory, J.M., R.J. Stouffer, S.C.B. Raper, P.A. Stott and N.A. Rayner, 2002. An observationally based estimate of the climate sensitivity. *J. Climate*, **15**: 3117-3121.

Hansen, J., M. Sato, L. Nazarenko, R. Ruedy, A. Lacis, D. Koch, I. Tegen, T. Hall, D. Shindell, B. Santer, P. Stone, T. Novakov, L. Thomason, R. Wang, Y. Wang, D. Jacob, S. Hollandsworth, L. Bishop, J. Logan, A. Thompson, R. Stolarski, J. Lean, R. Willson, S. Levitus, J. Antonov, N. Rayner, D. Parker and J. Christy, 2002. Climate forcings in

Goddard Institute for Space Studies SI2000 simulations. *J. Geophysical Research,* **107**(D18): 4347.

Hansen, J., G. Russell, D. Rind, P. Stone, A. Lacis, S. Lebedeff, R. Ruedy and L. Travis, 1983. Efficient three-dimensional global models for climate studies: Models I and II. *Monthly Weather Review*, **111**: 609-662.

Holian, G.L., A.P. Sokolov, and R.G. Prinn, 2001. *Uncertainty in Atmospheric CO_2 Predictions from a Global Ocean Carbon Cycle Model*. Report 80, MIT Joint Program on the Science and Policy of Global Change (http://mit.edu/globalchange/www/MITJPSPGC_Rpt80.pdf).

Holland, M.M., 2003. The North Atlantic Oscillation/Arctic Oscillation in the CCSM2 and its influence on Arctic climate variability. *J. Climate*, **16**: 2767-2781.

Huang, B., P.H. Stone, A.P. Sokolov and I.V. Kamenkovich, 2003a. The deep-ocean heat uptake in transient climate change. *J. Climate*, **16**: 1352–1363.

Huang, B., P.H. Stone, A.P. Sokolov and I.V. Kamenkovich, 2003b. Ocean heat uptake in transient climate change: Mechanisms and uncertainty due to subgrid-scale eddy mixing. *J. Climate*, **16**: 3344-3356.

IPCC (Intergovernmental Panel on Climate Change), 2001. *Climate Change 2000: The Scientific Basis*. Cambridge University Press, U.K.

Jones, P.D., and A. Moberg, 2003. Hemispheric and large-scale surface air temperature variations: An extensive revision and an update to 2001. *J. Climate*, **16**: 206-223.

Kamenkovich, I.V., A. Sokolov and P.H. Stone, 2003. Feedbacks affecting the response of the thermohaline circulation to increasing CO_2. A study with a model of intermediate complexity. *Climate Dynamics*, **21**(2): 119-130.

Kamenkovich, I.V., A. Sokolov and P.H. Stone, 2002. An efficient climate model with a 3D ocean and statistical-dynamical atmosphere. *Climate Dynamics,* **19**(7): 585-598.

Lean, J., 2000. Evolution of the sun's spectral irradiance since the Maunder Minimum. *Geophysical Research Letters*, **27**: 2421-2424.

Liu, Y., 1996. *Modeling the Emissions of Nitrous Oxide (N_2O) and Methane (CH_4) from the Terrestrial Biosphere to the Atmosphere*. Ph.D. Thesis, MIT. Joint Program on the Science and Policy of Global Change, Report 10, Cambridge, MA, 219p.

Marshall, J.C., C. Hill, L. Perelman and A. Adcroft, 1997a. Hydrostatic, quasi-hydrostatic and non-hydrostatic ocean modeling. *J. Geophysical Research*, **102**: 5733-5752.

Marshall, J.C., A. Adcroft, C. Hill, L. Perelman and C. Heisey, 1997b. A finite-volume, incompressible Navier-Stokes model for the studies of the ocean on parallel computers. *J. Geophysical Research*, **102**: 5,753-5,766.

Matear, R.J., and A.C. Hirst, 1999. Climate change feedback on the future oceanic CO_2 uptake. *Tellus B*, **51**: 722-733.

Matus, K., 2005. *Health Impacts from Urban Air Pollution in China: The Burden to the Economy and the Benefits of Policy*. Master's Thesis, Engineering Systems Division, Massachusetts Institute of Technology, Cambridge, MA.

Matus, K., T. Yang, S. Paltsev, J. Reilly, 2005. Economic benefits of air pollution regulation in the USA: An integrated approach. *Climatic Change*, in review (see also http://mit.edu/globalchange/www/MITJPSPGC_Rpt113.pdf).

Mayer, M., C. Wang, M. Webster and R. G. Prinn, 2000. Linking local air pollution to global chemistry and climate. *J. Geophysical Research*, **105**(D18): 22,869-22,896.

McFarland, J., J Reilly and H. Herzog, 2004. Representing energy technologies in top-down economic models using bottom-up information. *Energy Economics*, **26**(4): 685-707.

Meehl, G.A., W.M. Washington, J.M. Arblaster and A. Hu, 2004. Factors affecting climate sensitivity in global coupled models. *J. Climate*, **17**: 1584-1596.

Melillo, J.M., A.D. McGuire, D.W. Kicklighter, B. Moore III, C.J. Vorosmarty and A.L. Schloss, 1993. Global climate change and terrestrial net primary production. *Nature*, **363**: 234-240.

Millero, F., 1995. Thermodynamics of the carbon dioxide system in the oceans. *Geochemica et Cosmochimica Acta*, **59**: 661-677.

NAS (National Academy of Sciences), 1979. *Carbon Dioxide and Climate: A Scientific Assessment*. U.S. National Academy Press, Washington, D.C., 22p.

Olivier, J.G.J., and J.J.M. Berdowski, 2001. Global emission sources and sinks. In: *The Climate System,* J. Berdowski, R. Guicherit and B.J. Heij (eds.), Lisse: Swets & Zeitlinger Publishers. EDGAR 3.2 by RIVM/TNO, pp. 33-77.

Paltsev S., J. Reilly, H. Jacoby, R. Eckaus and J. McFarland and M. Babiker 2005a. *The MIT Emissions Prediction and Policy Analysis (EPPA) Model: Version 4*. MIT Joint Program on the Science and Policy of Global Change Report, forthcoming.

Paltsev S., H. Jacoby, J. Reilly, L. Viguier, and M. Babiker, 2005b. Modeling the Transport Sector: The Role of Existing Fuel Taxes in Climate Policy. In: *Energy and Environment*, R. Loulou, J.-P. Waaub, G. Zaccour (eds.), Springer, ISBN 0-387-25351-3 (see also http://mit.edu/globalchange/www/MITJPSPGC_Rpt117.pdf).

Paltsev, S., L. Viguier, M. Babiker, J. Reilly and K.H. Tay, 2004. *Disaggregating Household Transport in the MIT-EPPA Model*. Technical Note 5, MIT Joint Program on the Science and Policy of Global Change (available at http://mit.edu/globalchange/www/MITJPSPGC_TechNote113.pdf).

Parekh, P., M.J. Follows and E. Boyle, 2005. Decoupling of iron and phosphate in the global ocean. *Global Biogeochemical Cycles*, **19**, doi:10.1029/2004GB002280.

Petoukhov, V., M. Claussen, A. Berger, M. Crucifix, M. Eby, A. Eliseev, T. Fichefet, A. Ganopolski, H. Goosse, I. Kamenkovich, I. Mokhov, M. Montoya, L. A. Mysak, A. Sokolov, P. Stone, Z. Wang and A. Weaver, 2005. EMIC Intercomparison Project (EMIP-CO2): Comparative analysis of EMIC simulations of climate, and of equilibrium and transient responses to atmospheric CO_2 doubling. *Climate Dynamics*, in press .

Prinn, R. and J. Cohen, 2005. *An Efficient and Flexible Model of Urban Air Chemistry for Use in Climate and Human Health Studies*. MIT Joint Program on the Science and Policy of Global Change Report, forthcoming.

Prinn, R., J. Reilly, M. Sarofim, C. Wang and B. Felzer, 2005. Effects of air pollution control on climate. In: *Integrated Assessment of Human-induced Climate Change*, M. Schlesinger (ed.), Cambridge University Press, in press (see also http://mit.edu/globalchange/www/MITJPSPGC_Rpt118.pdf).

Prinn, R., H. Jacoby, A. Sokolov, C. Wang, X. Xiao, Z. Yang, R. Eckaus, P. Stone, D. Ellerman, J. Melillo, J. Fitzmaurice, D. Kicklighter, G. Holian and Y. Liu, 1999. Integrated global system model for climate policy assessment: Feedbacks and sensitivity studies. *Climatic Change*, **41**: 469-546.

Raper, C.S.B., J.M. Gregory and R.J. Stouffer, 2002. The role of climate sensitivity and ocean heat uptake on AOGCM transient temperature and thermal expansion response. *J. Climate*, **15**: 124-130.

Reilly, J., B. Felzer, S. Paltsev, J.M. Melillo, R.G. Prinn, C. Wang, A.P. Sokolov and X. Wang, 2004. The Economic Impact of Climate, CO_2, and Tropospheric Ozone Effects on Crop Yields in China, the U.S., and Europe. *Eos Transactions*, **85**(47), American Geophysical Union, Fall Meeting (San Francisco, Dec. 13-17) Supplement, Abstract 7314; B33A-0239.

Reilly, J., M. Mayer and J. Harnisch, 2002. The Kyoto Protocol and non-CO_2 greenhouse gases and carbon sinks. *Environmental Modeling and Assessment,* **7**(4): 217-229.

Reilly, J., R. Prinn, J. Harnisch, J. Fitzmaurice, H. Jacoby, D. Kicklighter, J. Mellilo, P. Stone, A. Sokolov and C. Wang, 1999. Multi-gas assessment of the Kyoto Protocol. *Nature*, **401**, 549-555.

Rodell, M., P.R. Houser, U. Jambor, J. Gottschalck, K. Mitchell, C.-J. Meng, K. Arsenault, B. Cosgrove, J. Radakovich, M. Bosilovich, J.K. Entin, J.P. Walker, D. Lohmann and D. Toll, 2004. The Global Land Data Assimilation System. *Bulletin of the American Meteorological Society*, **85**(3): 381-394.

Rosegrant, M.W., X. Cai and S.A. Cline, 2002. *World Water and Food to 2025: Managing Scarcity.* International Food Policy Research Institute, Washington, D.C.

Sarmiento, J.L., T.M.C. Hughes, R.J. Stouffer and S. Manabe, 1998. Simulated response of the ocean carbon cycle to anthropogenic climate warming. *Nature*, **393**: 245-249.

Sarofim, M., C.E. Forest, D.M. Reiner and J.M. Reilly, 2004. *Stabilization and Global Climate Policy*. Report 110, MIT Joint Program on the Science and Policy of Global Change (http://mit.edu/globalchange/www/MITJPSPGC_Rpt110.pdf).

Sato, M., J.E. Hansen, M.P. McCormick and J.B. Pollack, 1993. Stratospheric aerosol optical depths. *J. Geophysical Research*, **98**: 22,987-22,994.

Schlosser, C.A., and D.W. Kicklighter, 2005. *A Land Model System for Integrated Global Change Assessments*. MIT Joint Program on the Science and Policy of Global Change Report, forthcoming.

Smith, S.J, R. Andres, E. Conception and J. Lurz, 2004. *Historical Sulfur Dioxide Emissions 1850-2000: Methods and Results.* PNNL Research Report 14537, Pacific Northwest National Laboratory.

Sokolov, A.P., 2005. *Does Model Sensitivity to Changes in CO_2 Provide a Measure of Sensitivity to the Forcing of a Different Nature?* Report No. 119, MIT Joint Program on the Science and Policy of Global Change (http://mit.edu/globalchange/www/MITJPSPGC_Rpt119.pdf).

Sokolov, A., C.E. Forest and P.H. Stone, 2003. Comparing oceanic heat uptake in AOGCM transient climate change experiments. *J. Climate*, **16**: 1573-1582.

Sokolov, A., and P.H. Stone, 1998. A flexible climate model for use in integrated assessments. *Climate Dynamics*, **14**: 291-303.

Stone, P.H., 2004. Climate Prediction: The Limits of Ocean Models. In: *State of the Planet: Frontiers and Challenges in Geophysics*, R.S.J. Sparks and C.J. Hawksworth (eds.), American Geophysical Union Monograph Vol. 150: Washington, DC, pp. 259-267.

Stone, P.H., and M.-S. Yao, 1990. Development of a two-dimensional zonally averaged statistical-dynamical model. III: The parameterization of the eddy fluxes of heat and moisture. *J. Climate*, **3**: 726-740.

Stone, P.H., and M.-S. Yao, 1987. Development of a two-dimensional zonally averaged statistical-dynamical model. II: The role of eddy momentum fluxes in the general circulation and their parameterization. *J. Atmospheric Science*, **44**: 3769-3536.

Stouffer, R.J., J. Yin, J.M. Gregory, K.W. Dixon, M.J. Spelman, W. Hurlin, A.J. Weaver , E. Eby, G.M. Flato, H. Hasumi, A. Hu, J. Jungclause, I.V. Kamenkovich, A. Levermann, M. Montoya, S. Murakami, S. Nawrath, A. Oka, W.R. Peltier, D.Y. Bobitaille, A. Sokolov, G. Vettoretti and N. Weber, 2005. Investigating the causes of the response of the thermohaline circulation to past and future climate changes. *J. Climate,* in review.

Tatang, M.A., W. Pan, R.G. Prinn and G.J. McRae, 1997. An efficient method for parametric uncertainty analysis of numerical geophysical models. *J. Geophysical Research*, **102**: 21,925-21,932.

Trenberth, K.E., J.G. Olson and W.G. Large, 1989. A global ocean wind stress climatology based on ECMWF analyses. Technical Report NCAR/TN-338+STR, National Center for Atmospheric Research, Boulder, Colorado.

US EPA, 2002. *Emissions and Projections of Non-CO_2 Greenhouse Gases from Developing Countries: 1990 – 2020*. Office and Air and Radiations (February).

US EPA (Environmental Protection Agency), 2001. *Non-CO$_2$ Greenhouse Gas Emissions from Developed Countries: 1990-2010*. Office of Air and Radiations, EPA-430-R-01-007 (Dec.).

United Nations, 2001. *World Population Prospects: The 2000 Revision*. Data in digital form. Population Division, Department of Economic and Social Affairs.

Wang, D., 2005. *The Economic Impact of Global Climate and Tropospheric Ozone on World Agricultural Production*. Master's Thesis, Engineering Systems Division, Massachusetts Institute of Technology, Cambridge (May).

Wang, C., 2004. A modeling study on the climate impacts of black carbon aerosols. *J. Geophysical Research*, **109**(D03106), doi:10.1029/2003JD004084.

Wang, C., R.G. Prinn and A. Sokolov, 1998. A global interactive chemistry and climate model: Formulation and testing. *J. Geophysical Research*, **103**: 3399-3418.

Wang, Y., and D. Jacob, 1998. Anthropogenic forcing on tropospheric ozone and OH since preindustrial times. *J. Geophysical Research*, **103**: 31,123-31,135.

Wanninkhof, R., 1992. Relationship between wind speed and gas exchange over the ocean. *J. Geophysical Research*, **97**: 7373-7382.

Webster, M., C. Forest, J. Reilly, M. Babiker, D. Kicklighter, M. Mayer, R. Prinn, M. Sarofim, A. Sokolov, P. Stone and C. Wang, 2003. Uncertainty analysis of climate change and policy response. *Climatic Change*, **62**, 295-320.

Webster, M.D., M. Babiker, M. Mayer, J.M. Reilly, J. Harnisch, R. Hyman, M.C. Sarofim and C. Wang, 2002. Uncertainty in emissions projections for climate models. *Atmospheric Environment*, **36**: 3659-3670.

Winton, M., 2000: A reformulated three-layer sea ice model. *J. Atmospheric and Oceanic Technology,* **17**: 525-531.

Xiao, X., J.M. Melillo, D.W. Kicklighter, A.D. McGuire, R.G. Prinn, C. Wang, P.H. Stone and A. Sokolov, 1998. Transient climate change and net ecosystem production of the terrestrial biosphere. *Global Biogeochemical Cycles*, **12**: 345-360.

Xiao, X., D.W. Kicklighter, J.M. Melillo, A.D. McGuire, P.H. Stone and A.P. Sokolov, 1997. Linking a global terrestrial biogeochemical model and a 2-dimensional climate model: Implications for the global carbon budget. *Tellus B*, **49**: 18-37.

Yamanaka, Y., and E. Tajika, 1996. The role of the vertical fluxes of particulate organic matter and calcite in the oceanic carbon cycle: studies using an ocean biogeochemical circulation model. *Global Biogeochemical Cycles*, **10**: 361-382.

Yang, T., K. Matus, S. Paltsev and J. Reilly, 2005. *Economic Benefits of Air Pollution Regulation in the USA: An Integrated Approach*. Report 113, MIT Global Change Joint Program (http://mit.edu/globalchange/www/MITJPSPGC_Rpt113.pdf).

Yang, T., J. Reilly and S. Paltsev, 2005. Air Pollution Health Effects: Toward Integrated Assessment. In: *The Coupling of Climate and Economic Dynamics*, A. Haurie and L. Viguier (eds.), Springer, IGSN: 1-4020-3424-5, pp. 267-293.

Zeng, X., M. Shaikh, Y. Dai, R. E. Dickinson and R. Myneni, 2002. Coupling of the Common Land Model to the NCAR Community Climate Model. *J. Climate*, **15**: 1832-1854.

Zhuang, Q., J.M. Melillo, D.W. Kicklighter, R.G. Prinn, A.D. McGuire, P.A. Steudler, B.S. Felzer and S. Hu, 2004. Methane fluxes between terrestrial ecosystems and the atmosphere at northern high latitudes during the past century: A retrospective analysis with a process-based biogeochemistry model. *Global Biogeochemical Cycles*, **18**: GB3010, doi:10.1029/2004GB002239.

Zhaung, Q., A.D. McGuire, J.M. Melillo, J.S. Clein, R.J. Dargaville, D.W. Kicklighter, R.B. Myneni, J. Dong, V.E. Romanovsky, J. Harden and J.E. Hobbie, 2003. Carbon cycling in extratropical terrestrial ecosystems of the Northern Hemisphere during the 20th Century: A modeling analysis of the influences of soil thermal dynamics. *Tellus B*, **55**: 751-776.

REPORT SERIES of the MIT *Joint Program on the Science and Policy of Global Change*

Contact the Joint Program Office to request a copy. The Report Series is distributed at no charge.

REPORT SERIES of the MIT *Joint Program on the Science and Policy of Global Change*

Contact the Joint Program Office to request a copy. The Report Series is distributed at no charge.

Contact the Joint Program Office to request a copy. The Report Series is distributed at no charge.